NATIONAL ADVISORY COMMITTEE FOR AERONAUTICS

TECHNICAL NOTE

No. 1099

TWO-DIMENSIONAL WIND-TUNNEL INVESTIGATION OF SEALED 0.22-AIRFOIL-CHORD INTERNALLY BALANCED AILERONS OF DIFFERENT CONTOUR ON AN NACA 65(112)-213 AIRFOIL

By Albert L. Braslow

Langley Memorial Aeronautical Laboratory
Langley Field, Va.

Washington
July 1946

NATIONAL ADVISORY COMMITTEE FOR AERONAUTICS

TECHNICAL NOTE NO. 1099

TWO-DIMENSIONAL WIND-TUNNEL INVESTIGATION OF SEALED 0.22-AIRFOIL-CHORD INTERNALLY BALANCED AILERONS OF DIFFERENT CONTOUR ON AN NACA $65_{(112)}$-213 AIRFOIL

By Albert L. Braslow

SUMMARY

A two-dimensional wind-tunnel investigation was made of two interchangeable sealed 0.22-airfoil-chord internally balanced ailerons on an NACA $65_{(112)}$-213 airfoil. One of the ailerons tested was of true airfoil contour and the other was modified by partly eliminating the cusp near the trailing edge. Tests were made to determine the effects of the aileron contour modification on the section aerodynamic characteristics of the airfoil and aileron.

The results of the investigation indicated that the modification to the aileron contour caused the aileron effectiveness to increase slightly at low aileron deflections and to decrease slightly at large aileron deflections; caused the rate of change of aileron section hinge-moment coefficient with both section angle of attack and aileron deflection to increase positively; caused little change in the hinge-moment parameter for a given rate of roll at the low aileron deflections but an increase in the hinge-moment parameter for a given rate of roll at the high aileron deflections; caused no appreciable change in the section drag coefficient, rate of change of section lift coefficient with section angle of attack, and airfoil critical Mach number; and caused an increase of approximately 9 percent in the maximum section lift coefficient of the airfoil with the ailerons neutral. The application of standard roughness to the leading edge of the airfoil increased positively the rate of change of aileron section hinge-moment coefficient with both section angle of attack and aileron deflection, decreased the aileron effectiveness throughout the aileron deflection range, and caused a smaller change in the hinge-moment parameter for the true-contour aileron at any given rate of roll than for the modified aileron. Aileron deflections of -3° and 3° were found to have no significant effect on the airfoil critical Mach number at the design section lift coefficient.

INTRODUCTION

Thickening the cusped trailing edge of low-drag airfoils is sometimes desirable, mainly for structural reasons. Enough experimental data are not available at present to show how to thicken the cusp to best advantage, but a method of thickening this part of the airfoil by straight-line fairings has been shown during previous investigations to alter the aerodynamic characteristics of some low-drag airfoils. In an attempt to keep changes in the aerodynamic characteristics at a minimum, a compromise modification was made to the cusp of an NACA $65_{(112)}$-213 airfoil by retaining the original airfoil mean line while fairing out the upper surface to a straight line.

The effect of the contour modification on the aileron effectiveness and hinge moments and on the airfoil drag characteristics and critical Mach number were determined from an investigation in the Langley two-dimensional low-turbulence pressure tunnel of the NACA $65_{(112)}$-213 airfoil equipped with two interchangeable sealed 0.22-airfoil-chord internally balanced ailerons; one of true airfoil contour and one of the modified contour. Tests were made with the airfoil surfaces aerodynamically smooth and with standard roughness applied to the leading edge. In addition, the differential pressures across the aileron seals were obtained for use in estimating the hinge-moment characteristics of the ailerons with any amount of sealed internal balance.

COEFFICIENTS AND SYMBOLS

The coefficients and symbols used in the presentation of results are defined as follows:

c_l airfoil section lift coefficient $(l/q_o c)$

$c_{l_{max}}$ airfoil maximum section lift coefficient

c_d airfoil section drag coefficient $(d/q_o c)$

$\Delta p/q_o$ seal-pressure-difference coefficient; positive when pressure below seal is greater than pressure above seal

c_h aileron section hinge-moment coefficient based on aileron chord $(h/q_o c_a^2)$

c_H aileron section hinge-moment coefficient based on airfoil chord $(h/q_o c^2)$

S airfoil pressure coefficient $\left(\frac{H_o - p}{q_o}\right)$

where

l airfoil lift per unit span

d airfoil drag per unit span

h aileron hinge moment per unit span; positive when trailing edge of aileron tends to deflect downward

c chord of airfoil with aileron neutral

c_a chord of aileron behind hinge axis

q_o free-stream dynamic pressure $\left(\frac{1}{2}\rho_o V_o^2\right)$

V_o free-stream velocity

ρ_o free-stream density

H_o free-stream total pressure

p local static pressure

and

α_o airfoil section angle of attack, degrees

δ_a aileron deflection with respect to airfoil, degrees; positive when trailing edge is deflected downward

c_b chord of overhang from aileron hinge axis to middle of gap seal

R Reynolds number

M_{cr} airfoil critical Mach number

$$c_{l_\alpha} = \left(\frac{\partial c_l}{\partial \alpha_o}\right)_{\delta_a}$$

$$c_{l_\delta} = \left(\frac{\partial c_l}{\partial \delta_a}\right)_{\alpha_o}$$

$$c_{h_\alpha} = \left(\frac{\partial c_h}{\partial \alpha_o}\right)_{\delta_a}$$

$c_{h_\delta} = \left(\frac{\partial c_h}{\partial \delta_a}\right)_{\alpha_o}$

$P_\alpha = \left(\frac{\partial \frac{\Delta p}{q_o}}{\partial \alpha_o}\right)_{\delta_a}$

$P_\delta = \left(\frac{\partial \frac{\Delta p}{q_o}}{\partial \delta_a}\right)_{\alpha_o}$

α_δ aileron section effectiveness parameter $\left(\frac{\partial \alpha_o}{\partial \delta_a}\right)_{c_l}$

$\Delta\alpha_o$ increment of airfoil section angle of attack

$\Delta\delta_a$ increment of aileron deflection

$\left(\frac{\Delta\alpha_o}{\Delta\delta_a}\right)_{c_l}$ aileron section effectiveness parameter; ratio of increment of airfoil section angle of attack to increment of aileron deflection required to maintain constant section lift coefficient

$c_{h_{\delta_T}}$ total $dc_h/d\delta_a$ in steady roll

n aileron response parameter

$(\Delta c_h)_\delta$ increment of aileron section hinge-moment coefficient due to aileron deflection at constant section angle of attack

$(\Delta c_h)_\alpha$ increment of aileron section hinge-moment coefficient due to change in section angle of attack at constant aileron deflection

Δc_{H_T} increment of total aileron section hinge-moment coefficient in steady roll

$\frac{\Delta c_{H_T}}{\Delta\alpha_o/\Delta\delta_a}$ aileron section hinge-moment parameter

The subscripts to partial derivatives denote the variables held constant when the partial derivatives are measured. The derivatives are measured at zero angle of attack and zero aileron deflection.

MODEL

The model had a 24-inch chord and was constructed of laminated mahogany with the exception of the interchangeable ailerons, which were constructed of cast aluminum. The two ailerons tested, which had chords of 0.22c and sealed internal balances of approximately $0.33c_a$, differed only in contour. One was of true airfoil contour (NACA $65_{(112)}$-213) and the other was modified by the partial elimination of the cusp near the trailing edge. The modification consisted of fairing out the upper-surface cusp near the trailing edge with a straight line from a point 0.133c above the trailing edge tangent to the airfoil contour and modifying the lower surface so as to retain the original airfoil mean line. Ordinates of the basic NACA $65_{(112)}$-213 airfoil section are given in table I and the ordinates for the rear 30 percent of the modified airfoil are given in table II. Sketches of the two ailerons are given as figure 1. Rubber seals were used along the complete span and at both ends of the ailerons to stop the flow of air through the gaps.

For the smooth condition of the model, the airfoil surfaces were sanded with No. 400 carborundum paper to produce an aerodynamically smooth finish. For the standard airfoil leading-edge roughness condition, the model surfaces were aerodynamically smooth except that 0.011-inch carborundum grains were applied to each airfoil surface at the leading edge over a surface length of 0.08c measured from the leading edge (reference 1).

APPARATUS AND TESTS

Tests of the model with each of the two ailerons were made in the Langley two-dimensional low-turbulence pressure tunnel. The tests included measurements at a Reynolds number of 8×10^6 of airfoil lift and drag, aileron hinge moment, and balance pressure for the aerodynamically smooth model with various deflections of each aileron. Airfoil lift, aileron hinge-moment, and balance-pressure characteristics were also determined at a Reynolds number of 8×10^6 for the model with standard roughness applied to the leading edge and with various deflections of each aileron. With each aileron neutral, lift and drag measurements were made of the model both in an aerodynamically smooth condition and with standard leading-edge roughness at Reynolds numbers of 2×10^6, 6×10^6, 8×10^6,

and 9×10^6, corresponding to Mach numbers of 0.15, 0.14, 0.15, and 0.17, respectively. In addition, airfoil surface pressures were measured from the leading edge to 0.70c at a Reynolds number of 8×10^6 through an approximate range of section lift coefficient from -0.5 to 1.0 with the ailerons neutral and at the design section lift coefficient of 0.20 with the ailerons deflected -3° and 3°.

Lift and drag measurements were made by the methods briefly described in reference 1. Airfoil surface pressures and the pressure difference across the aileron seals were measured with static-pressure orifices located along both airfoil surfaces and in the chamber above and below the aileron balance plate. Aileron hinge-moment measurements were made with a pressure-bellows balance.

The following factors were applied to correct the tunnel data to free-air conditions:

$$c_l = 0.977c_l'$$

$$c_d = 0.992c_d'$$

$$q_o = 1.008q_o'$$

$$\alpha_o = 1.015\alpha_o'$$

where the primed quantities represent the values measured in the tunnel (reference 1).

RESULTS AND DISCUSSION

The basic section lift, drag, hinge-moment, and balance-pressure data are presented in figures 2 to 6 for the true-contour aileron and in figures 7 to 11 for the modified aileron. These figures include data for the airfoil with aerodynamically smooth surfaces and with standard roughness applied to the leading edge. The discussion of the data refers to that obtained at a Reynolds number of 8×10^6 unless otherwise stated.

Aileron Effectiveness

The effects of the aileron contour modification on the aileron section effectiveness parameter α_δ and on c_{l_δ} are

shown in table III and curves of α_o against δ_a at a constant c_l of 0.20 are shown in figure 12. For the airfoil in an aerodynamically smooth condition, the effectiveness parameter α_δ is slightly greater for the modified aileron than for the true-contour aileron. The values of α_δ for the modified and true-contour ailerons are 97 percent and 94 percent, respectively, of the thin-airfoil theoretical effectiveness (reference 2) and 17 percent and 12 percent, respectively, greater than the value (-0.430) obtained on the NACA 0009 airfoil section (reference 3). Standard airfoil leading-edge roughness caused a larger adverse effect on the effectiveness of the modified aileron than on the effectiveness of the true-contour aileron.

In order to show the variation of the aileron effectiveness with lift coefficient and aileron deflection, values of the effectiveness have been measured between definite aileron deflections at a constant section lift coefficient and are designated $\left(\Delta\alpha_o/\Delta\delta_a\right)_{c_l}$. Values of $\left(\Delta\alpha_o/\Delta\delta_a\right)_{c_l}$ are shown plotted against section lift coefficient in figure 13 for aileron-deflection limits of $\pm10^\circ$ and $\pm20^\circ$. The effectiveness of the modified aileron is slightly greater than that of the true-contour aileron on the aerodynamically smooth airfoil when measured between aileron deflections of -10° and 10°. An increase in the aileron-deflection limits to -20° and 20° causes a larger reduction in the effectiveness of the modified than of the true-contour aileron with the result that the true-contour aileron is slightly more effective at the high aileron deflections. For the airfoil with standard roughness applied to the leading edge, the values of $\left(\Delta\alpha_o/\Delta\delta_a\right)_{c_l}$ for the true-contour aileron were higher than for the modified aileron when measured between aileron deflections of both $\pm10^\circ$ and $\pm20^\circ$.

Aileron Hinge Moments

The aileron hinge moments and balance pressures were measured when the airfoil angle of attack α_o was both increased and decreased. The values of c_h and $\Delta p/q_o$ were generally found to be more positive for increasing than for decreasing angles of attack. The total variation usually amounted to less than 0.006 and 0.06 for c_h and $\Delta p/q_o$, respectively. It is felt reasonably certain that this difference in the values of c_h and $\Delta p/q_o$ was caused by a lag in aileron setting as the angle of attack was changed due to the method used in attaching the ailerons to the pressure-bellows balance and also by friction in the control-surface and hinge-moment balance bearings. Average values

of the section hinge-moment coefficient and seal-pressure-difference coefficient are used, therefore, in the presentation of results.

Section characteristics.- The variations of aileron section hinge-moment coefficient c_h and seal-pressure-difference coefficient $\Delta p/q_c$ with airfoil section angle of attack α_o are presented in figures 5 and 6 for the true-contour aileron and in figures 10 and 11 for the modified aileron. The irregularities that occur in the variation of c_h with α_o for the smooth airfoil correspond to the limits of the low-drag range as shown in figures 3 and 8. Similar irregularities have been noted during other two-dimensional investigations of control surfaces (for example, reference 4) and are believed to be caused by the sudden movements in transition along the airfoil surfaces at the extremities of the low-drag range. Reference 4 indicates that no unusual aileron stick-force characteristics will be caused by the sudden changes in the two-dimensional hinge-moment coefficients. The addition of standard roughness to the airfoil leading edge eliminated the irregularities as shown in figures 5(b) and 10(b).

Values of c_{h_α}, c_{h_δ}, P_α, and P_δ for both ailerons on the smooth and rough airfoils are given in table III. The modification to the aileron contour or standard airfoil leading-edge roughness caused small positive increases in both c_{h_α} and c_{h_δ}. The variation of c_h and $\Delta p/q_o$ with δ_a at a constant section lift coefficient of 0.20 is presented in figure 12.

The basic section hinge-moment and balance-pressure data of figures 5, 6, 10, and 11 may be used to estimate the section hinge-moment characteristics of ailerons of similar contour and chord with any amount of sealed internal balance by the method given in reference 5.

Basis for comparison.- The mean angle of attack at which an aileron is operating is altered by the rate of roll. The effect of the change in angle of attack on the aileron hinge-moment characteristics must be taken into account for comparison of ailerons from section data. This correction is usually made by use of the constant-lift concept, in which the assumption is made that the aileron part of the wing acts at constant lift during steady roll. The rate of change of the section hinge-moment coefficient with aileron deflection in steady roll is then given by the equation

$$c_{h_{\delta_T}} = c_{h_\delta}\left(1 + \frac{\partial \alpha_o}{\partial \delta_a}\frac{c_{h_\alpha}}{c_{h_\delta}}\right) \qquad (1)$$

British research, however, has indicated that the parameter c_{h_α} is overstressed in the constant-lift concept and that a more accurate equation is

$$c_{h_{\delta_T}} = c_{h_\delta}\left(1 - n\frac{c_{h_\alpha}}{c_{h_\delta}}\right) \tag{2}$$

where n is a response parameter dependent upon the aileron dimensions, wing aspect ratio and taper, and spanwise location of the aileron. A typical value of n, equal to 0.2, is given in a British paper of limited distribution but more recent NACA data indicate that a more suitable value of n for the ailerons of a modern fighter-type airplane is 0.27, and that value has been used in the present analysis. Equation (2) is inadequate for determining the three-dimensional aileron characteristics, but it may be used for comparing the two ailerons of different contour. In order to apply equation (2) to non-linear curves it has been converted to increments of the total aileron section hinge-moment coefficient in steady roll by

$$\Delta c_{H_T} = \left(\frac{c_a}{c}\right)^2 \left\{\left(\Delta c_h\right)_\delta \left[1 - \frac{n}{\Delta\alpha_o/\Delta\delta_a}\frac{\left(\Delta c_h\right)_\alpha}{\left(\Delta c_h\right)_\delta}\right]\right\} \tag{3}$$

The method of analysis is the same as that used in reference 6. The hinge-moment parameter $\frac{\Delta c_{H_T}}{\Delta\alpha_o/\Delta\delta_a}$, which is the ratio of the increment of section hinge-moment coefficient in steady roll to the aileron effectiveness, is plotted against the equivalent change in section angle of attack $\Delta\alpha_o$ required to maintain a constant section lift coefficient for various deflections of the aileron from neutral. This method of analysis takes into account the aileron effectiveness and hinge moment and the possible mechanical advantage between the controls and the ailerons. The aileron span and possible three-dimensional-flow effects are not considered except as indicated in equation (3). The smaller the value of the hinge-moment parameter for a given value of $\Delta\alpha_o$, the more advantageous the combination should be for providing a lower control force for a given value of the wing-tip helix angle.

Aileron comparison.- Values of the hinge-moment parameter $\frac{\Delta c_{H_T}}{\Delta\alpha_o/\Delta\delta_a}$ are plotted against $\Delta\alpha_o$ in figure 14 for each aileron

on the airfoil in a smooth condition and with standard roughness applied to the leading edge. For the smooth airfoil, both ailerons should provide about the same control force at low aileron deflections. The true-contour aileron should provide the lower control force at high aileron deflections for the airfoil in a smooth condition and through the entire range of deflections tested for the airfoil with standard leading-edge roughness. Although the application of standard roughness generally causes the value of the hinge-moment parameter to increase slightly for any given value of $\Delta\alpha_o$ (fig. 14), the control force for the true-contour aileron would change less with changes in the surface condition of the wing, as can be seen from a comparison of the values of $\frac{\Delta c_{H_T}}{\Delta\alpha_o/\Delta\delta_a}$ for the smooth airfoil with those for the airfoil with standard leading-edge roughness.

Lift

The modification to the aileron contour or standard airfoil leading-edge roughness had no effect on the airfoil lift-curve slope with the aileron neutral as shown in table III. The value of c_{l_α} is equal to 0.104 for all conditions.

A comparison of figures 2 and 7 shows that the aileron contour modification increases appreciably the maximum section lift coefficient $c_{l_{max}}$ of the airfoil in a smooth condition. With the ailerons neutral the contour modification increases the value of $c_{l_{max}}$ from 1.37 for the true-contour aileron to 1.49. For the airfoil with standard leading-edge roughness, the aileron contour modification causes no significant change in $c_{l_{max}}$. The reduction in the value of $c_{l_{max}}$ caused by standard leading-edge roughness is similar to the decrease found for other NACA 65-series airfoils of comparable thickness (reference 1).

The effect of Reynolds number between 2×10^6 and 9×10^6 on the section lift characteristics of the airfoil in the smooth and rough conditions is shown in figures 4 and 9 for the neutral position of the true-contour and modified ailerons, respectively. Similar effects of Reynolds number are noted for the two ailerons. An increase in Reynolds number from 2×10^6 to 6×10^6 causes a large increase in maximum section lift coefficient for the smooth airfoil; however, a further increase in Reynolds number to 9×10^6 causes no appreciable change. For the airfoil with standard leading-edge roughness, Reynolds number through the range investigated has no significant effect on the value of $c_{l_{max}}$.

Drag

The aileron contour modification has no significant effect on the smooth airfoil section drag characteristics except at an aileron deflection of 20° as can be seen by comparing figure 3 for the true-contour aileron with figure 8 for the modified aileron. The values of the section drag coefficients for the 20° deflection of the modified aileron are doubtful, however, because of probable cross-flow along the span of the model. With the exception of the 20° deflection, a low-drag "bucket" was realized at all deflections of both ailerons.

The effect of increasing the Reynolds number from 2×10^6 to 9×10^6 was normal, that is, the value of the minimum section drag coefficient and the range of section lift coefficient for low-drag values decreased with increasing Reynolds number (figs. 4 and 9). The increase in the values of c_d caused by standard airfoil leading-edge roughness (figs. 4 and 9) is similar to that of other NACA 65-series airfoils of comparable thickness (reference 1).

Airfoil Pressure Distribution and Critical Mach Number

The pressure coefficients over both airfoil surfaces from the leading edge to 0.70c are presented in figure 15 through an approximate range of section lift coefficient from -0.5 to 1.0 for the airfoil with a neutral position of both the true-contour and modified ailerons. The variation of airfoil critical Mach number M_{cr}, estimated by von Kármán's method from the experimental surface pressures (reference 7), with section lift coefficient is presented in figure 16. The modification to the aileron contour had very little effect on the values of M_{cr}. Theoretical values of M_{cr} for the NACA 65(112)-213 airfoil section, calculated by the methods of reference 1, are also presented in figure 16. Good agreement exists between the values of M_{cr} predicted from theory and from the experimental data in the range of section lift coefficient for high critical Mach number and low drag.

The chordwise variation of airfoil pressure coefficient at approximately the design section lift coefficient of 0.20 is presented in figure 17 for the airfoil with each aileron deflected -3°, 0°, and 3°. Because the value of M_{cr} is a direct function of the peak pressure on the airfoil surface, the close agreement in the peak values of S for the aileron deflections tested indicate a negligible effect of an aileron deflection of -3° or 3°

on the airfoil critical Mach number at a constant section lift coefficient of 0.20.

CONCLUSIONS

A two-dimensional wind-tunnel investigation was made of an NACA $65_{(112)}$-213 airfoil equipped with two interchangeable sealed 0.22-airfoil-chord internally balanced ailerons of different contour. One of the ailerons tested was of true airfoil contour and the other was modified by the partial elimination of the cusp near the trailing edge. The data obtained indicated the following conclusions:

1. Modification of aileron contour caused

   (a) The aileron effectiveness to increase slightly at low aileron deflections and to decrease slightly at high aileron deflections

   (b) The rate of change of aileron section hinge-moment coefficient with both section angle of attack and aileron deflection to increase positively

   (c) Little change in the hinge-moment parameter for a given rate of roll at the low aileron deflections but an increase in the hinge-moment parameter for a given rate of roll at the high aileron deflections

   (d) No appreciable change in the section drag coefficient, rate of change of section lift coefficient with section angle of attack, and airfoil critical Mach number

   (e) An increase of approximately 9 percent in the maximum section lift coefficient of the airfoil with the ailerons neutral

2. The application of standard roughness to the leading edge of the airfoil

   (a) Increased positively the rate of change of aileron section hinge-moment coefficient with both section angle of attack and aileron deflection

   (b) Decreased the aileron effectiveness throughout the aileron deflection range

(c) Caused a smaller change in the hinge-moment parameter for the true-contour aileron at any given rate of roll than for the modified aileron

3 Aileron deflections of -3° and 3° had no significant effect on the airfoil critical Mach number at the design section lift coefficient of 0.20.

Langley Memorial Aeronautical Laboratory
National Advisory Committee for Aeronautics
Langley Field, Va , March 1, 1946

REFERENCES

1. Abbott, Ira H., von Doenhoff, Albert E., and Stivers, Louis S., Jr.: Summary of Airfoil Data. NACA ACR No. L5C05, 1945.

2. Glauert, H.: Theoretical Relationships for an Aerofoil with Hinged Flap. R. & M. No. 1095, British A.R.C., 1927.

3. Ames, Milton B., Jr., and Sears, Richard I.: Determination of Control-Surface Characteristics from NACA Plain-Flap and Tab Data. NACA Rep. No. 721, 1941.

4. Braslow, Albert L.: Two-Dimensional Wind-Tunnel Investigation of Low-Drag Vertical-Tail, Horizontal-Tail, and Wing Sections Equipped with Sealed Internally Balanced Control Surfaces. NACA TN No. 1048, 1946.

5. Fischel, Jack: Hinge Moments of Sealed-Internal-Balance Arrangements for Control Surfaces. II - Experimental Investigation of Fabric Seals in the Presence of a Thin-Plate Overhang. NACA ARR No. L5F30a, 1945.

6. Underwood, William J., Braslow, Albert L., and Cahill, Jones F.: Two-Dimensional Wind-Tunnel Investigation of 0.20-Airfoil-Chord Plain Ailerons of Different Contour on an NACA 65_1-210 Airfoil Section. NACA ACR No. L5F27, 1945.

7. von Kármán, Th.: Compressibility Effects in Aerodynamics. Jour. Aero. Sci., vol. 8, no. 9, July 1941, pp. 337-356.

TABLE I

ORDINATES FOR NACA $65_{(112)}$-213 AIRFOIL SECTION

[Stations and ordinates given in percent of airfoil chord]

Upper Surface		Lower Surface	
Station	Ordinate	Station	Ordinate
0	0	0	0
.423	1.042	.583	-.942
.658	1.262	.842	-1.129
1.146	1.617	1.354	-1.383
2.383	2.212	2.617	-1.842
4.867	3.133	5.133	-2.504
7.363	3.858	7.638	-3.008
9.863	4.462	10.138	-3.429
14.867	5.438	15.133	-4.092
19.883	6.183	20.117	-4.592
24.896	6.750	25.104	-4.958
29.917	7.163	30.083	-5.217
34.938	7.433	35.062	-5.371
39.958	7.567	40.042	-5.425
44.979	7.538	45.021	-5.350
50.000	7.338	50.000	-5.133
55.017	6.958	54.983	-4.767
60.033	6.425	59.967	-4.283
65.046	5.775	64.954	-3.717
70.054	5.025	69.946	-3.083
75.058	4.208	74.942	-2.417
80.054	3.333	79.946	-1.742
85.050	2.438	84.950	-1.092
90.038	1.542	89.962	-.508
95.017	.700	94.983	-.071
100.000	0	100.000	0

TABLE II

ORDINATES FOR REAR 30 PERCENT OF MODIFIED NACA $65_{(112)}$-213 AIRFOIL SECTION

[Stations and ordinates given in percent of airfoil chord]

Station	Ordinate	
	Upper surface	Lower surface
70.000	5.029	-3.058
75.000	4.225	-2.429
80.000	3.400	-1.792
85.000	2.592	-1.233
90.000	1.771	-.708
95.000	.946	-.300
100.000	.133	-.133

TABLE III

SECTION PARAMETERS MEASURED AT $\alpha_o = 0^\circ$ AND $\delta_a = 0^\circ$ FOR $R = 8 \times 10^6$

Surface (1)	c_{l_α}	c_{l_δ}	α_δ	c_{h_α}	c_{h_δ}	P_α	P_δ
True-contour aileron							
Smooth	0.104	0.059	-0.540	-0.0038	-0.0081	0.036	0.095
Rough	.104	.053	-.505	-.0035	-.0067	.029	.086
Modified aileron							
Smooth	0.104	0.060	-0.560	-0.0031	-0.0077	0.042	0.082
Rough	.104	.051	-.490	-.0027	-.0065	.029	.073

[1] "Smooth" and "Rough" refer to the airfoil with aerodynamically smooth surfaces and with standard leading-edge roughness.

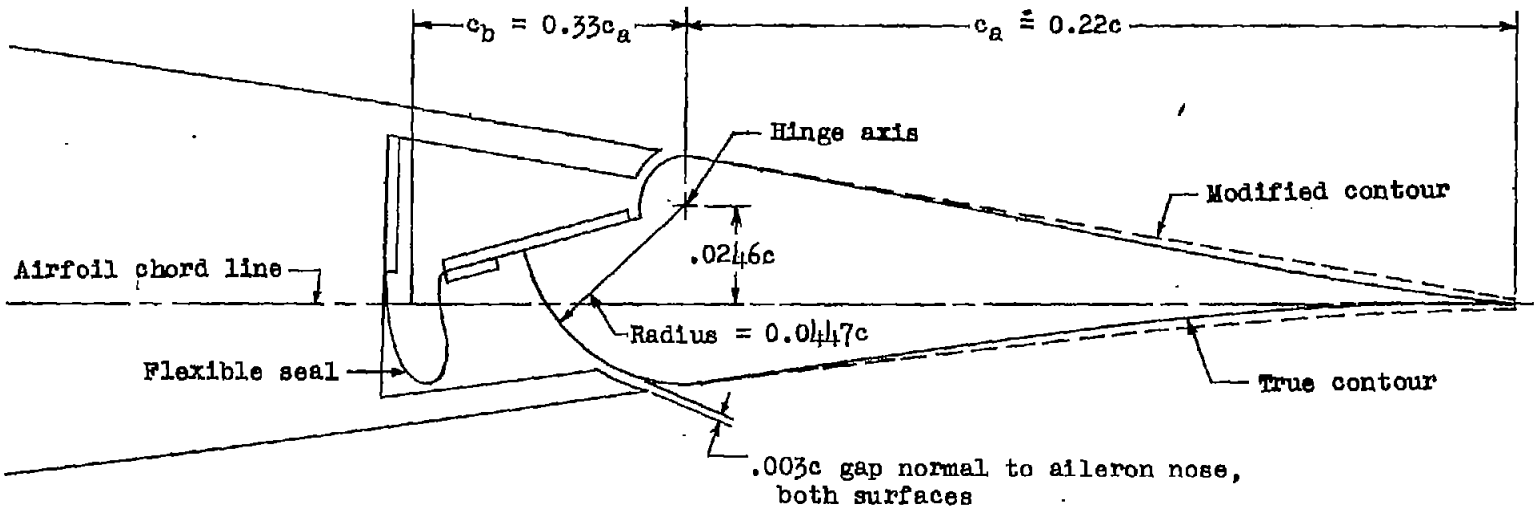

NATIONAL ADVISORY
COMMITTEE FOR AERONAUTICS

Figure 1.- Ailerons on the NACA $65_{(112)}$-213 airfoil section.

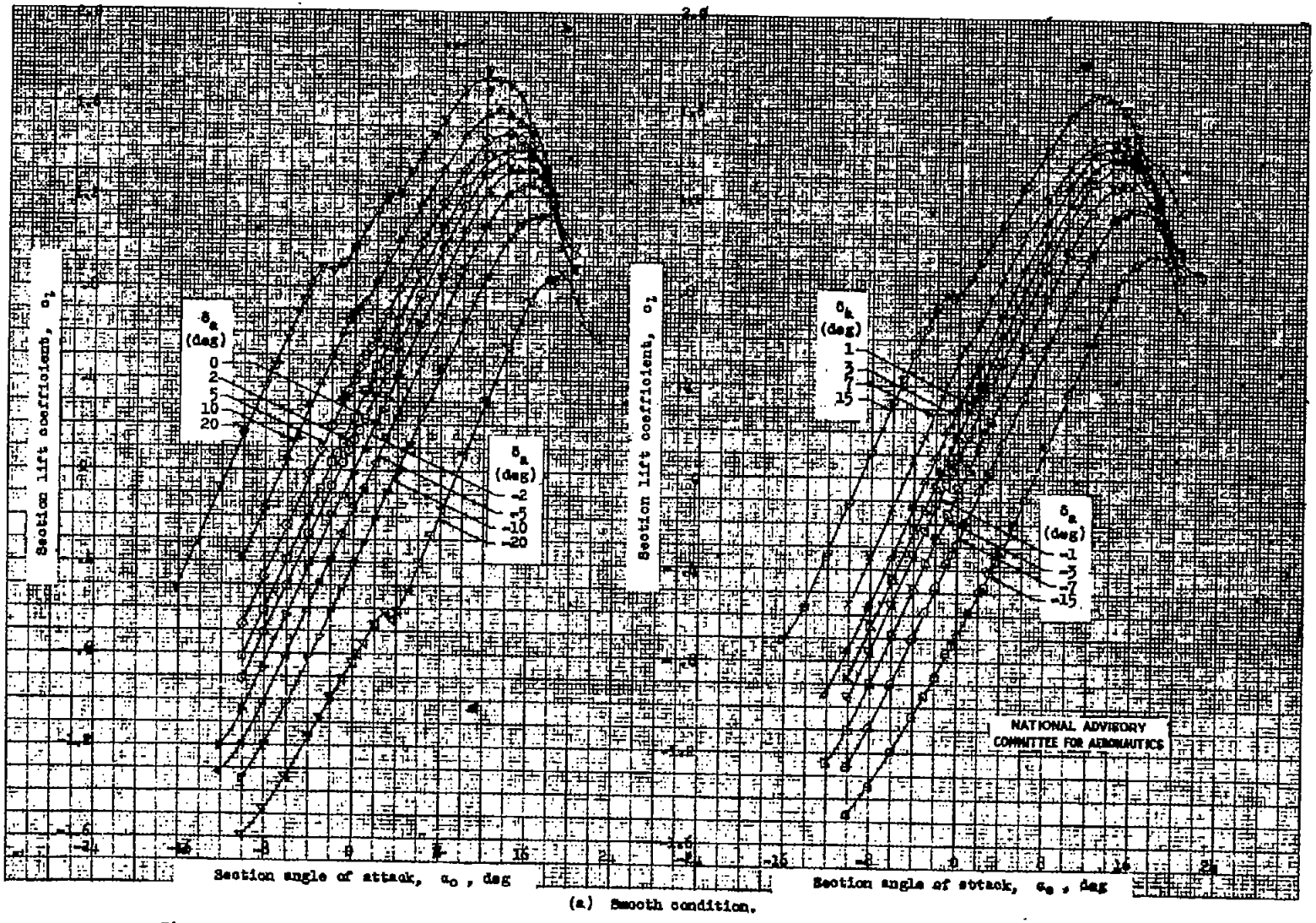

(a) Smooth condition.

Figure 2 .- Lift characteristics of an NACA $65_{(112)}$-213 airfoil section equipped with a sealed 0.22c internally balanced aileron of true airfoil contour. $R = 8 \times 10^6$; tests, TDT 696 and 708.

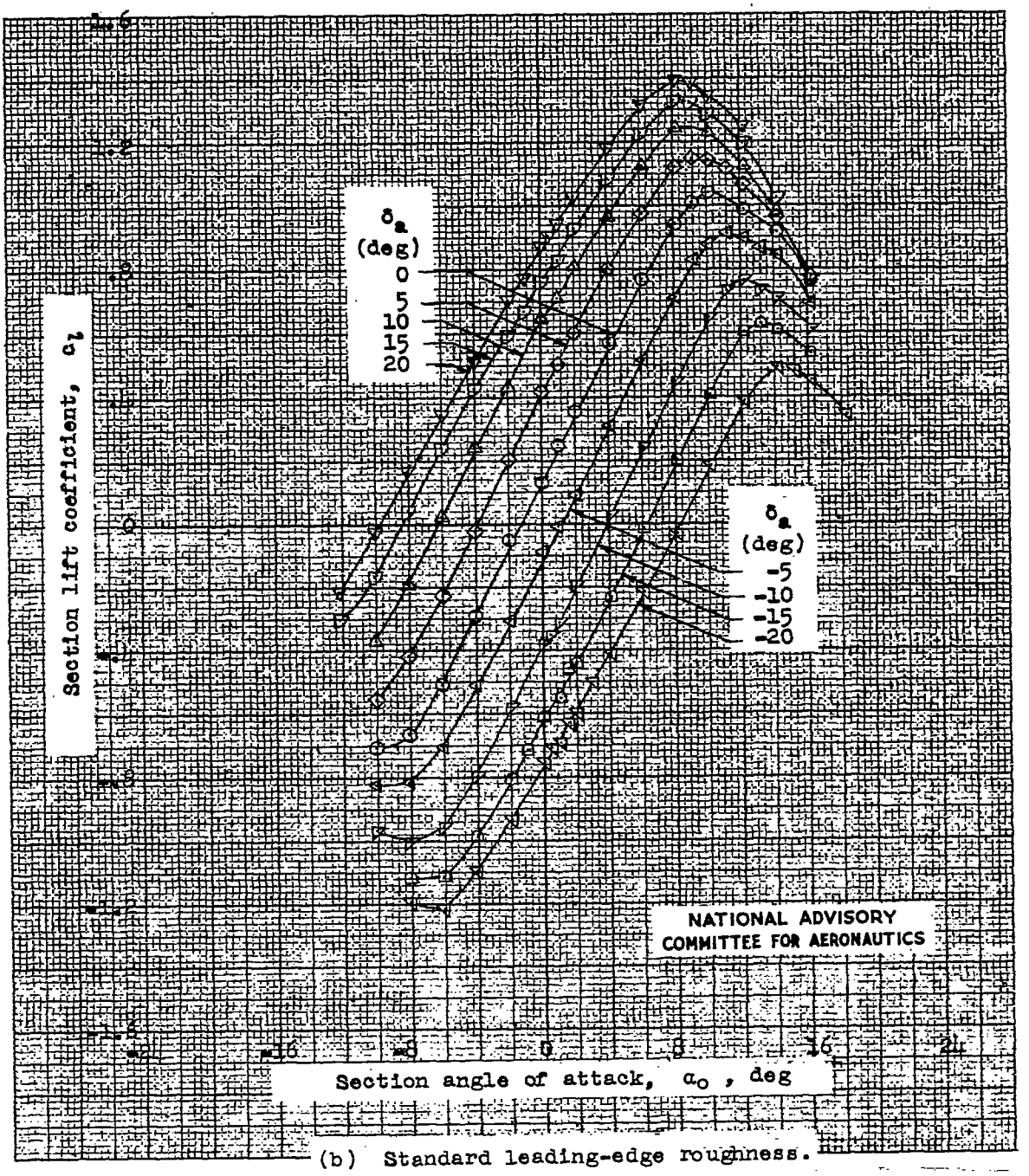

(b) Standard leading-edge roughness.

Figure 2 .- Concluded.

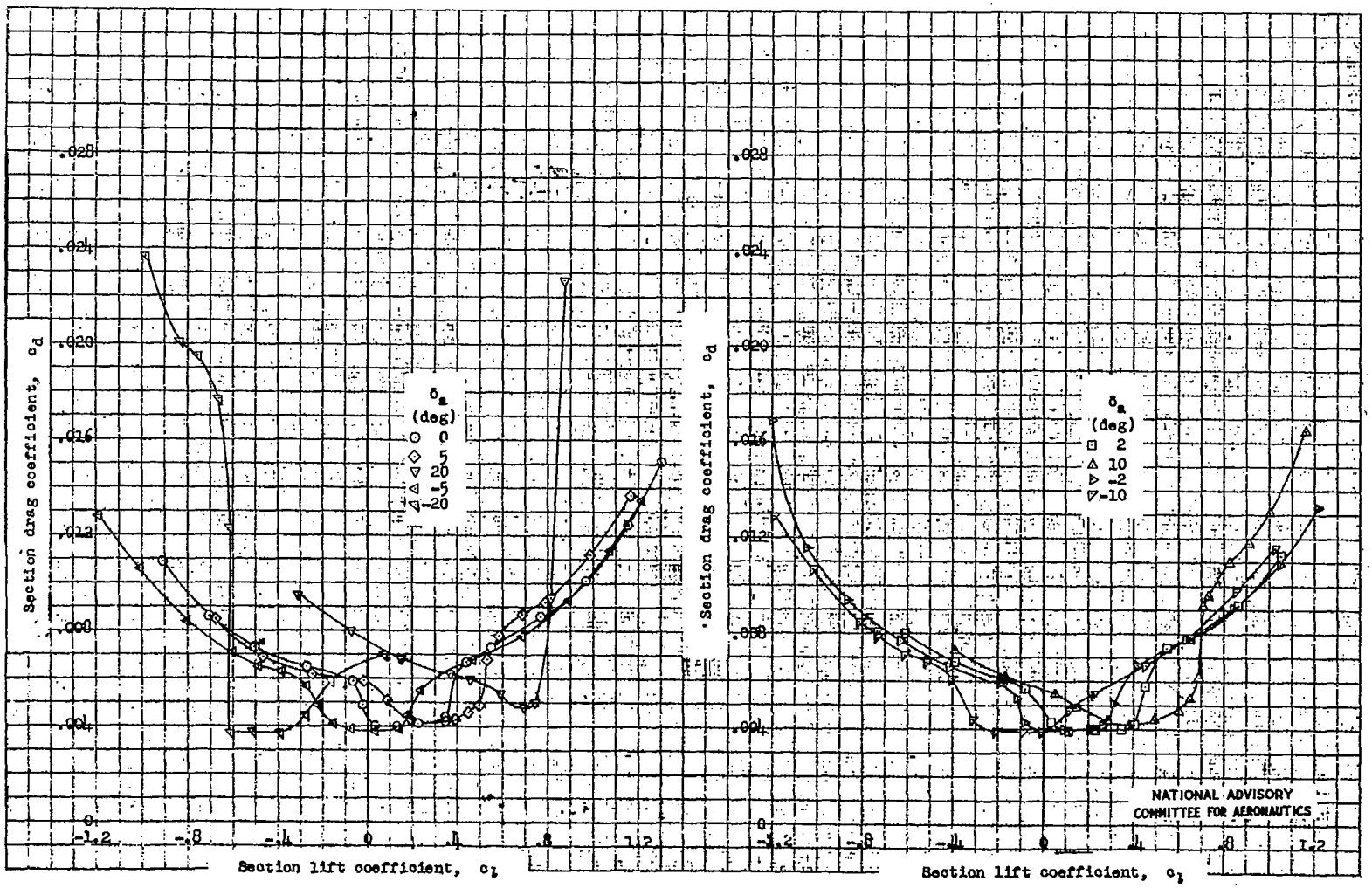

(a) Smooth condition.

Figure 3 .- Drag characteristics of an NACA $65_{(112)}$-213 airfoil section equipped with a sealed 0.22c internally balanced aileron of true airfoil contour, $R = 8 \times 10^6$; test, TDT 696.

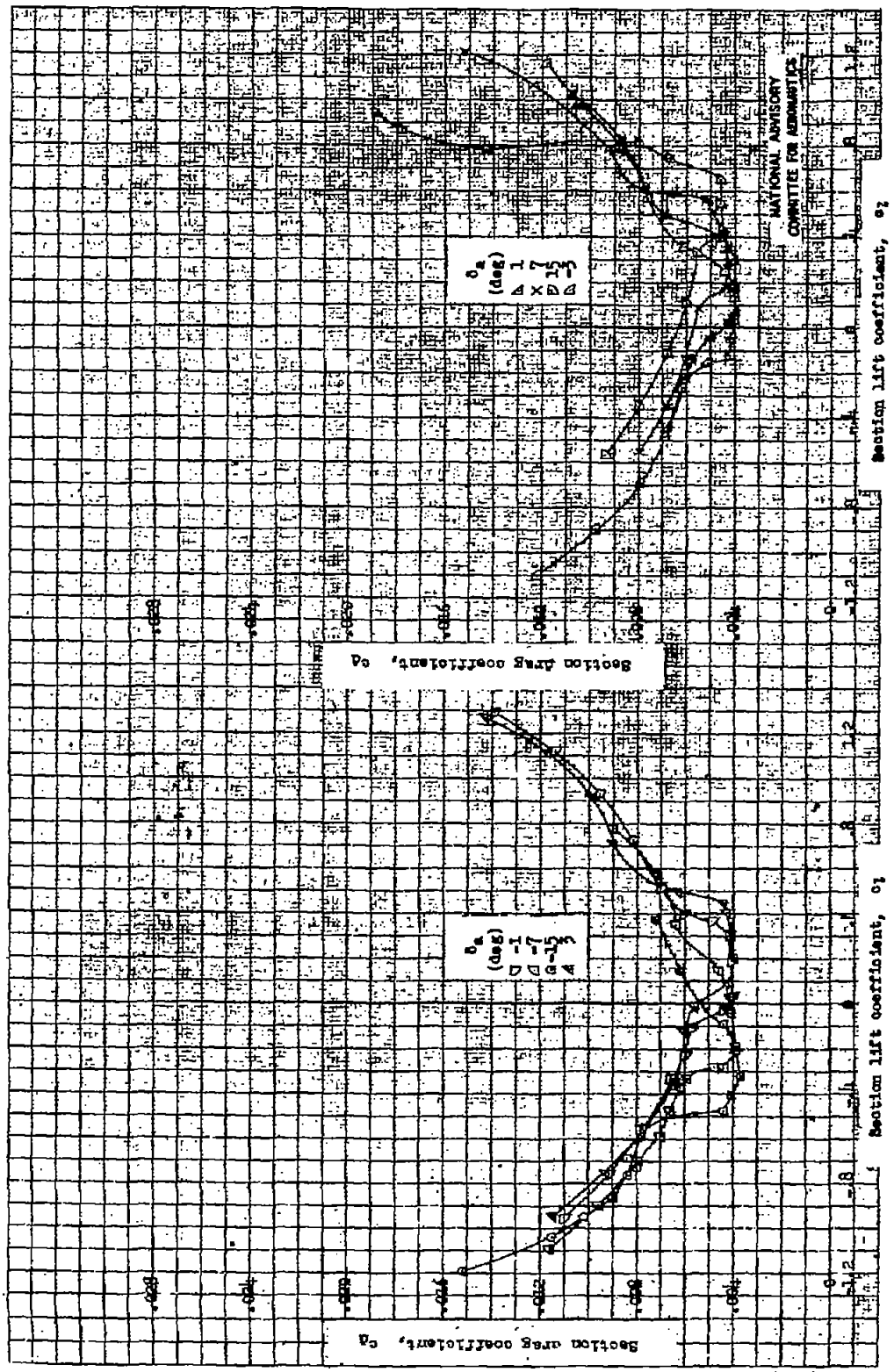

(b) Smooth condition (concluded).

Figure 3.- Concluded.

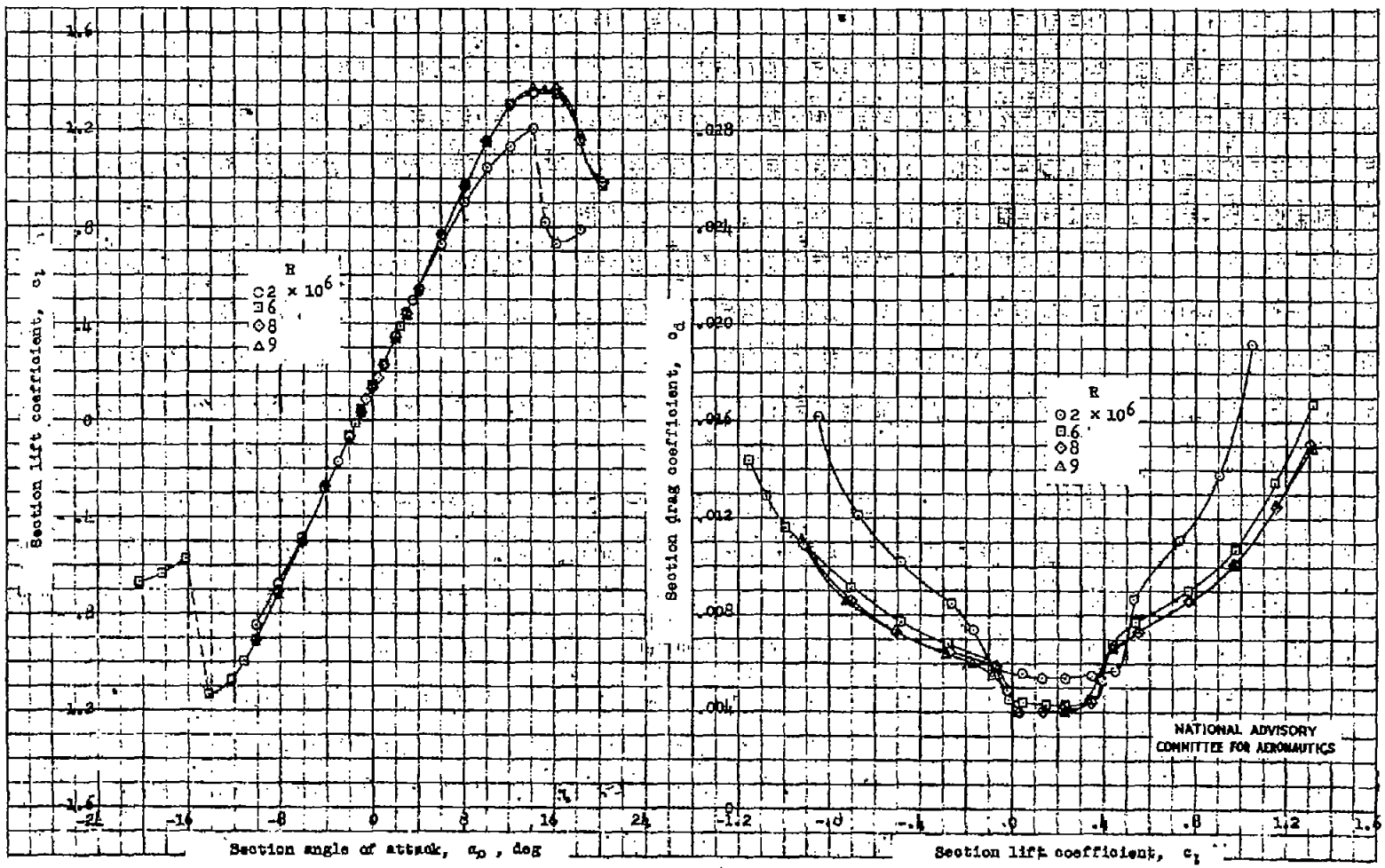

(a) Smooth condition.

Figure 4 .- Lift and drag characteristics of an NACA $65_{(112)}$-213 airfoil section equipped with a sealed 0.22c internally balanced aileron of true airfoil contour. $\delta_a = 0°$; tests, TDT 695, 696, and 708.

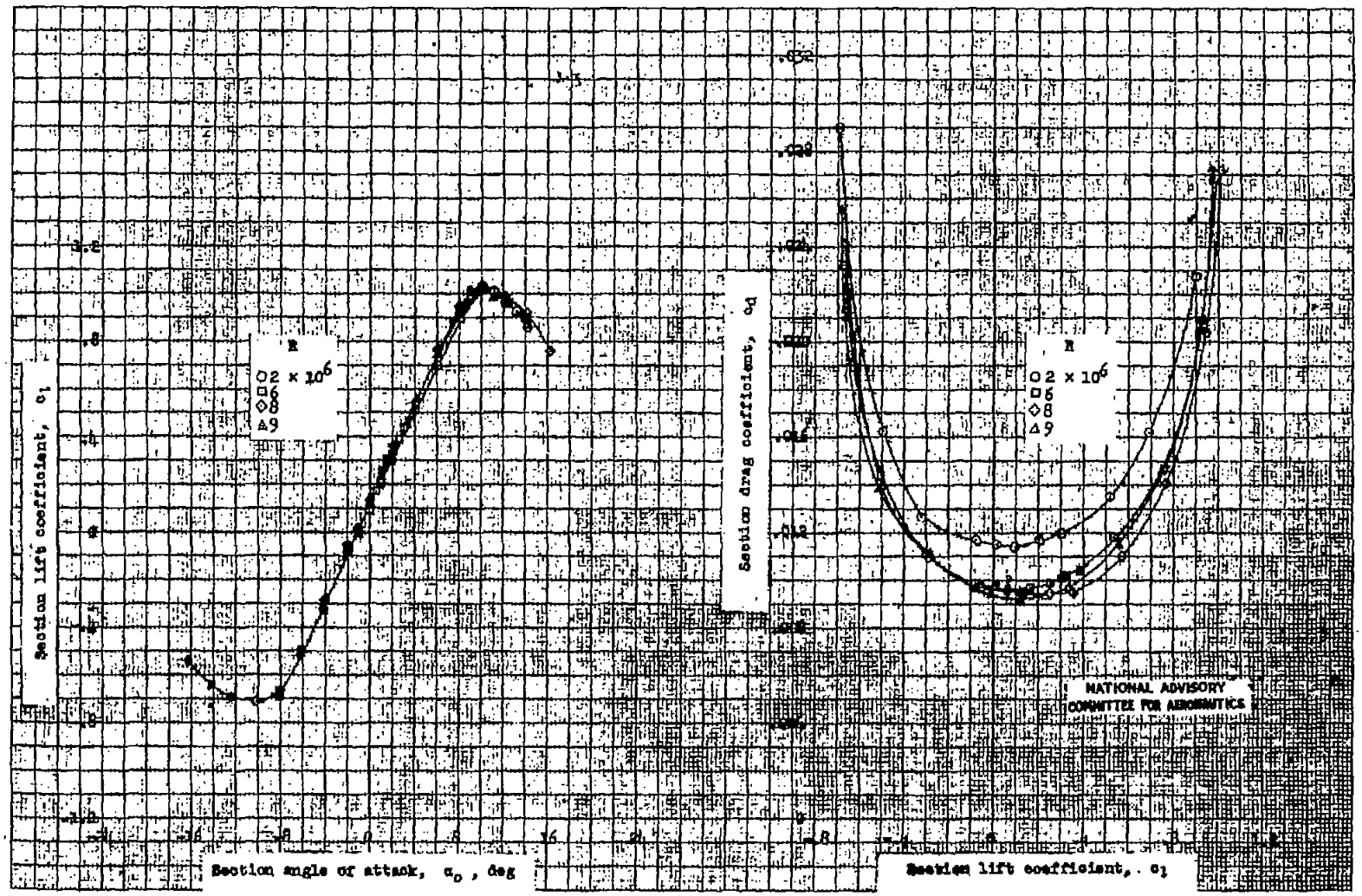

(b) Standard leading-edge roughness.

Figure 4 .- Concluded.

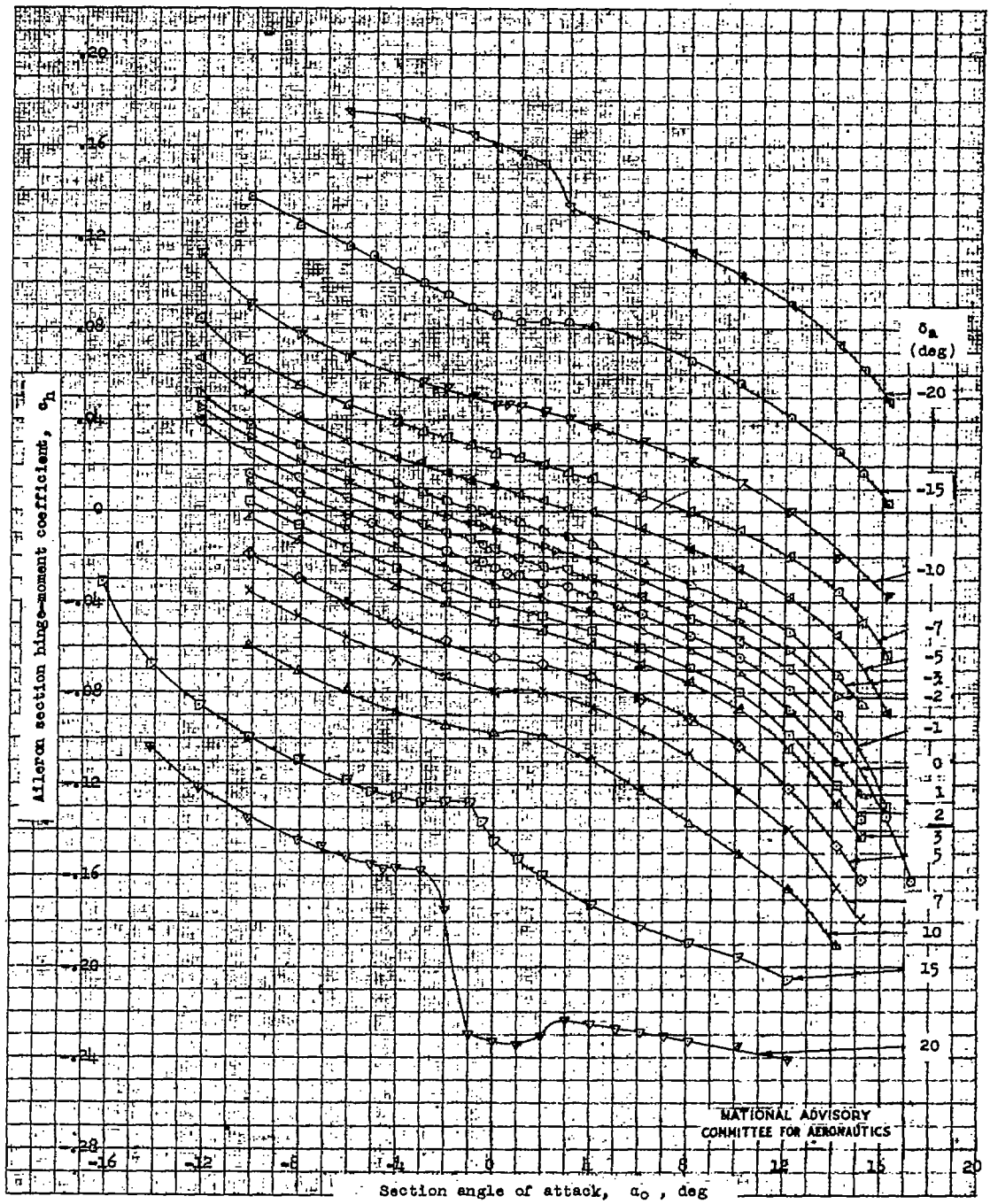

(a) Smooth condition.

Figure 5 .- Hinge-moment characteristics of a sealed 0.22c internally balanced aileron of true airfoil contour on an NACA $65_{(112)}$-213 airfoil section. R = 8 × 10^6; test, TDT 708.

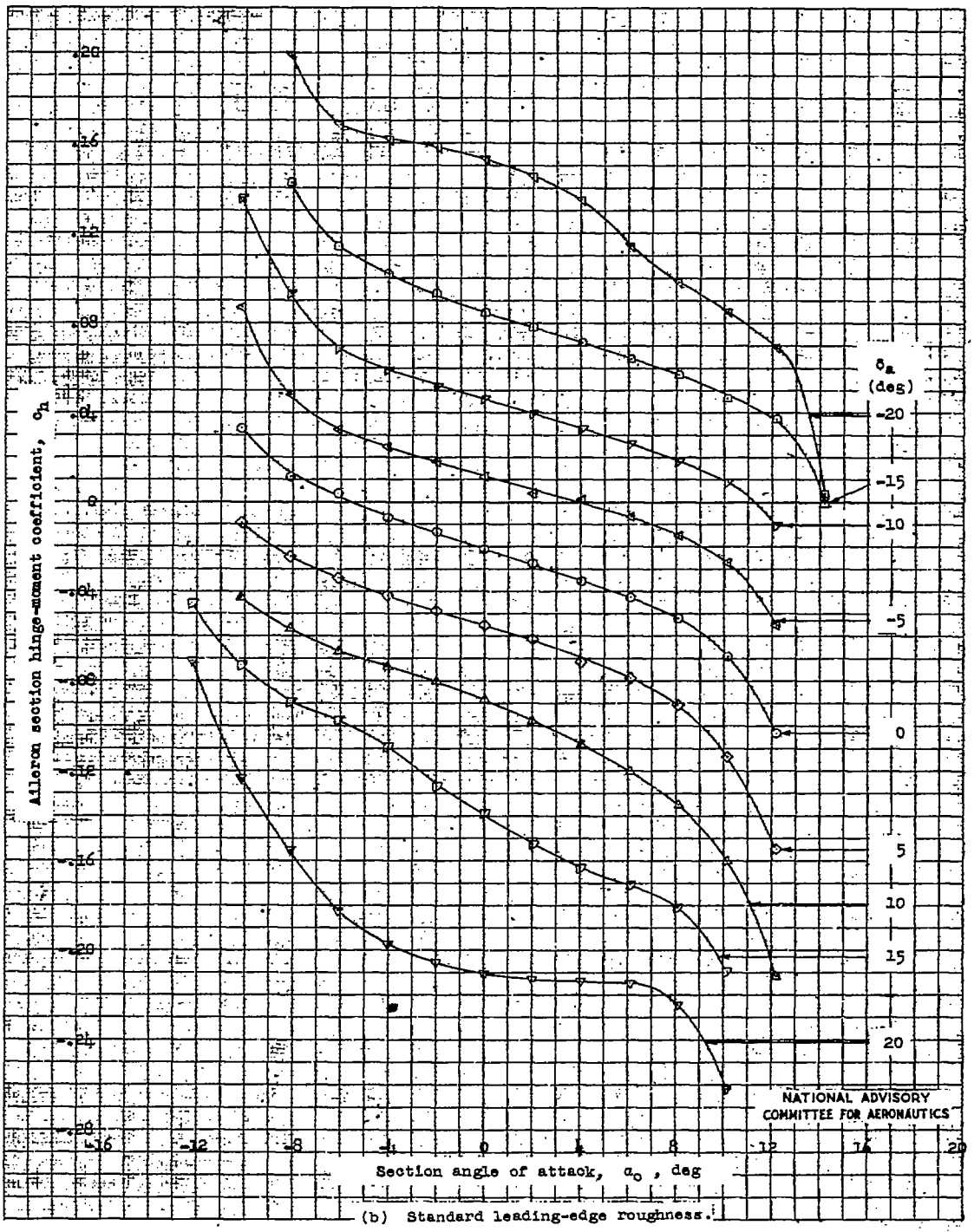

(b) Standard leading-edge roughness.

Figure 5 .- Concluded.

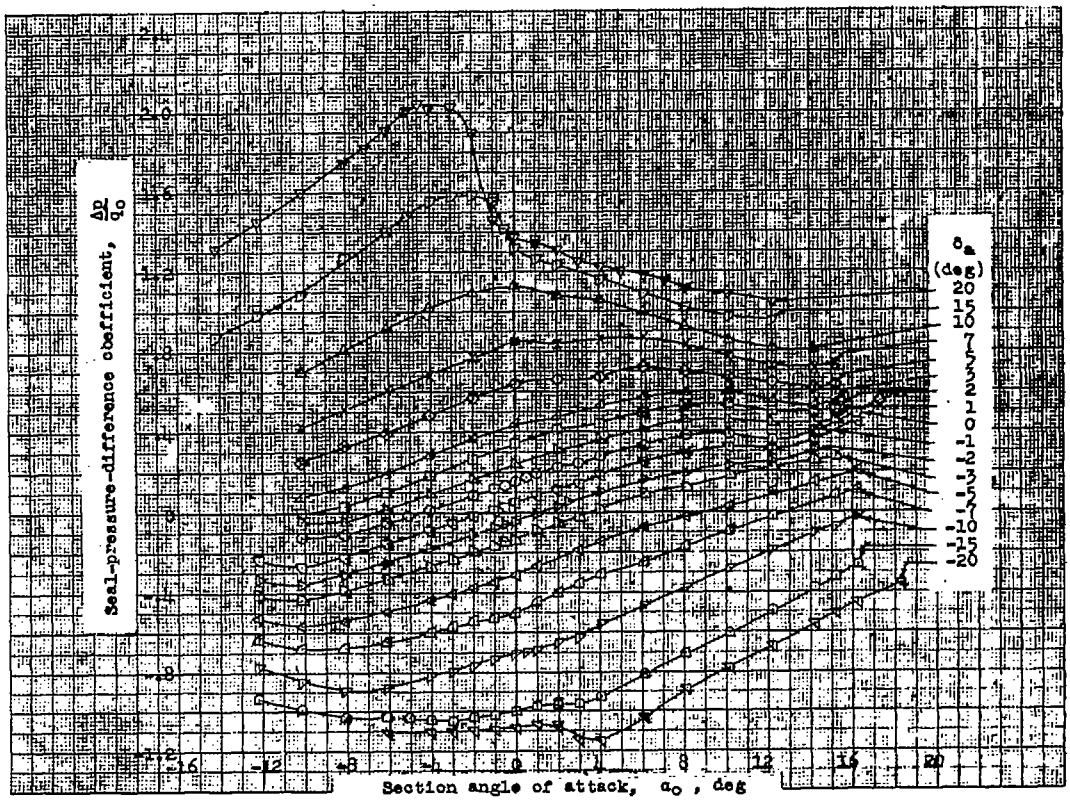

(a) Smooth condition.

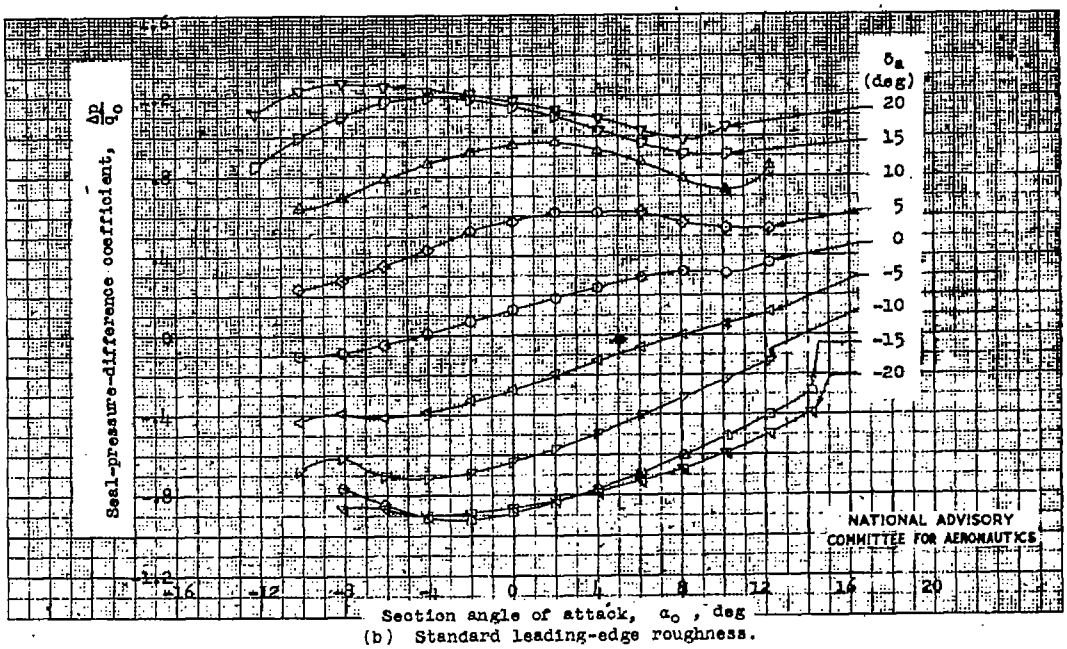

(b) Standard leading-edge roughness.

Figure 6.- Variation of $\frac{\Delta p}{q_o}$ with α_o for a sealed 0.22c internally balanced aileron of true airfoil contour on an NACA 65(112)-213 airfoil section. $R = 8 \times 10^6$; TDT 708.

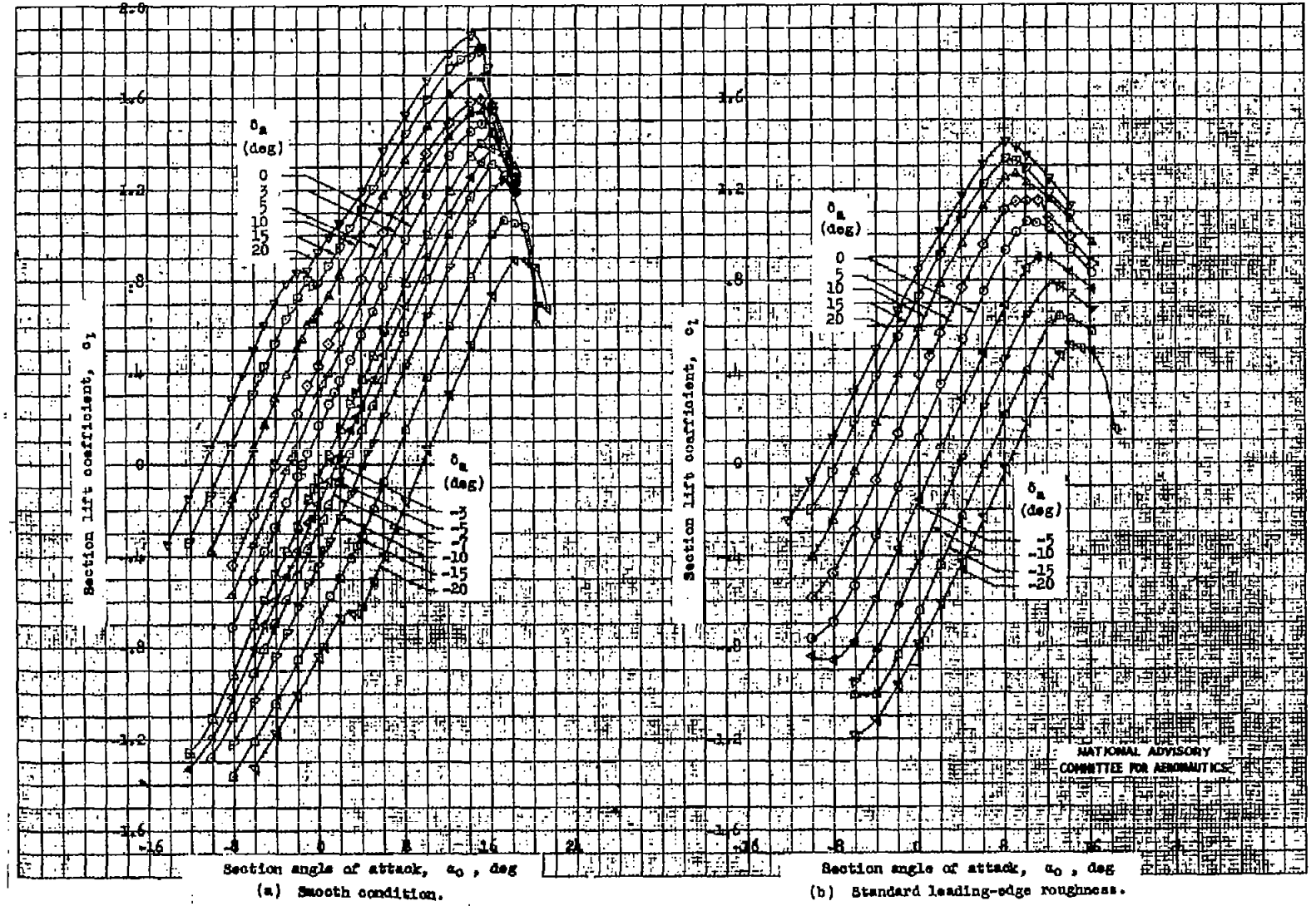

(a) Smooth condition.

(b) Standard leading-edge roughness.

Figure 7 .- Lift characteristics of an NACA $65_{(112)}$-213 airfoil section equipped with a sealed 0.22c internally balanced aileron of modified contour. $R = 8 \times 10^6$; tests, TDT 701 and 711.

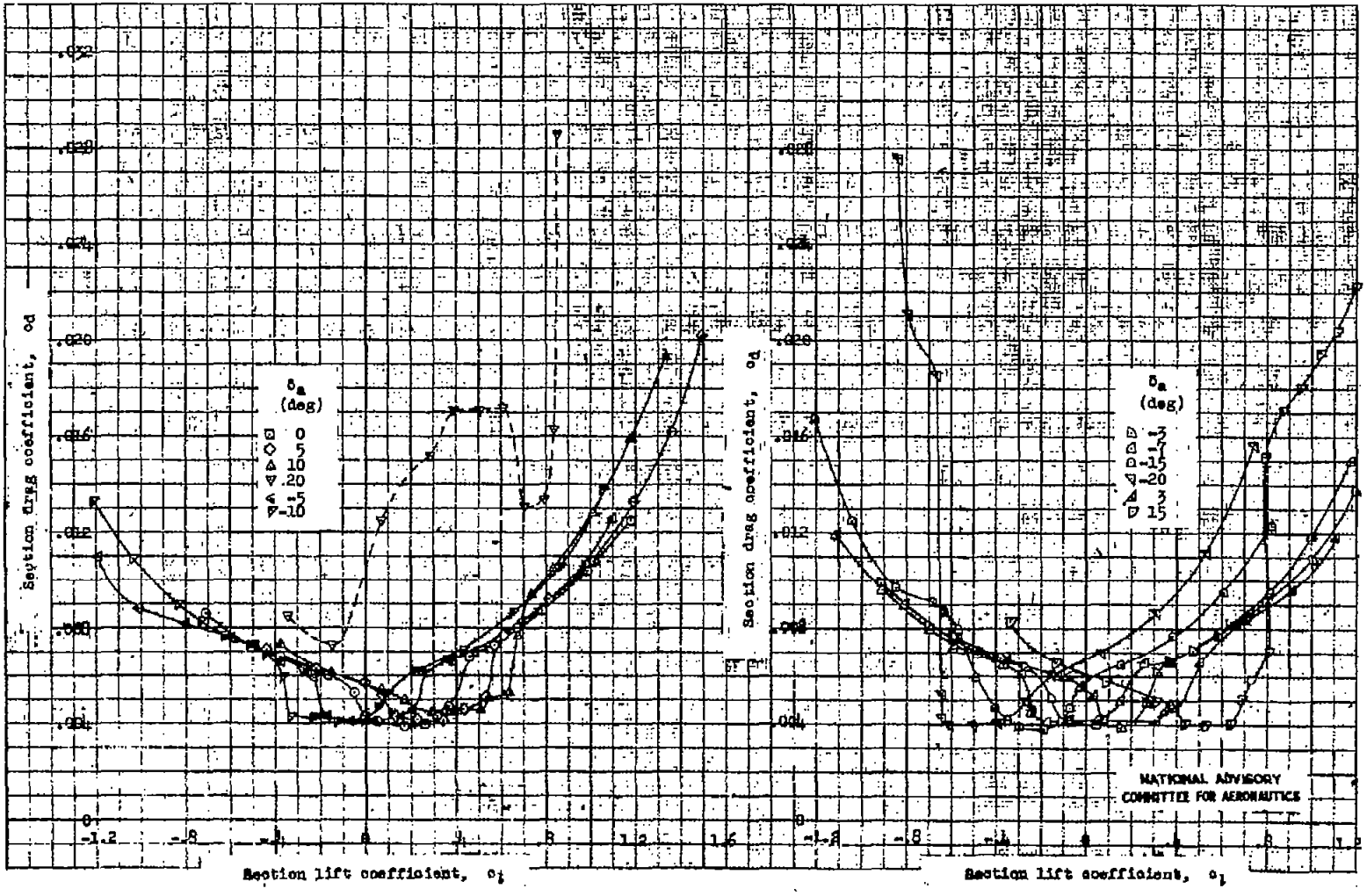

Figure 8 .- Drag characteristics of an NACA $65_{(112)}$-213 airfoil section equipped with a sealed 0.22c internally balanced aileron of modified contour. $R = 8 \times 10^6$; smooth condition; test, TDT 701.

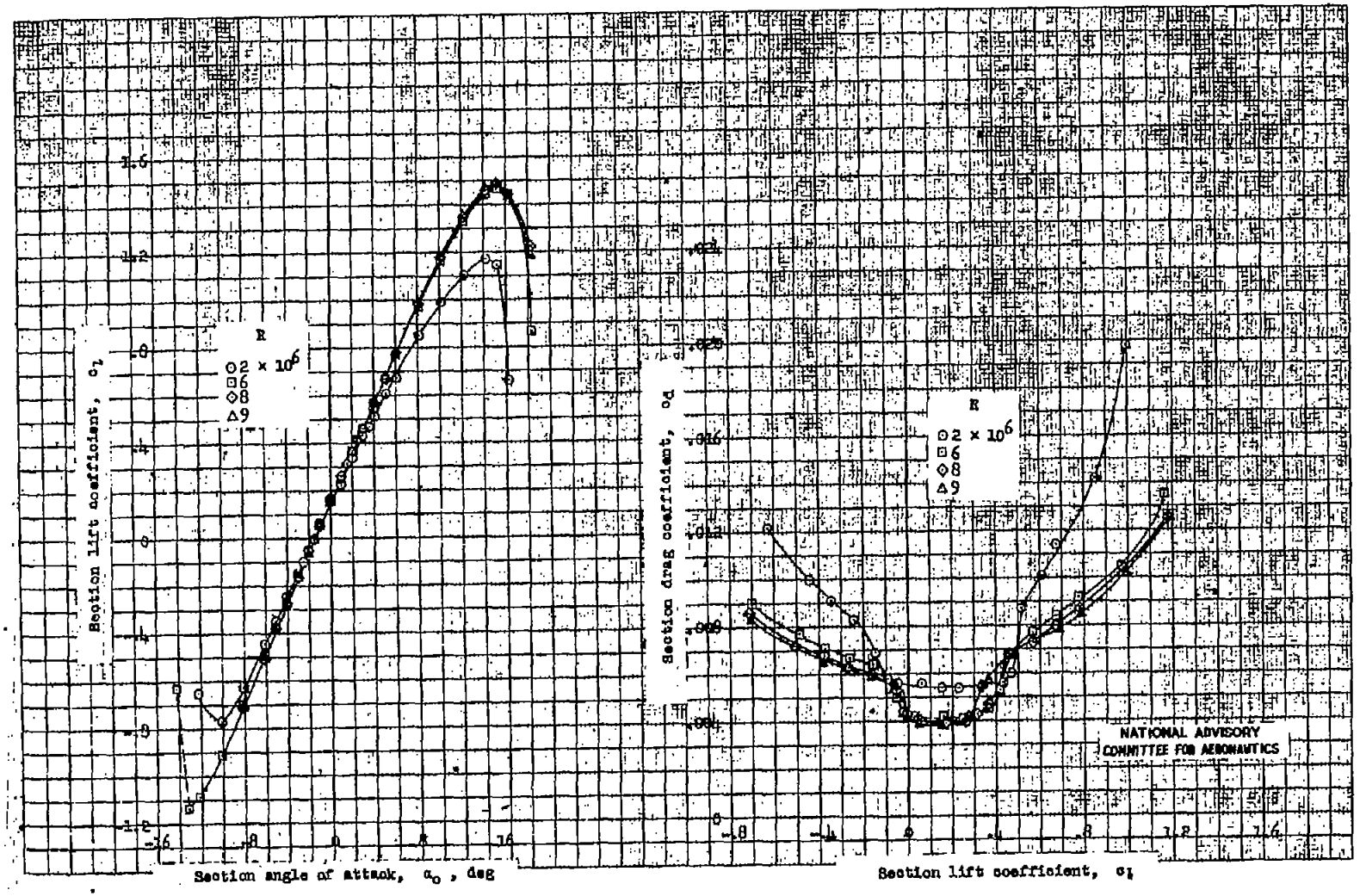

(a) Smooth condition.

Figure 9 .- Lift and drag characteristics of an NACA $65_{(112)}$-213 airfoil section equipped with a sealed 0.22c internally balanced aileron of modified contour. $\delta_a = 0°$; tests, TDT 701 and 703.

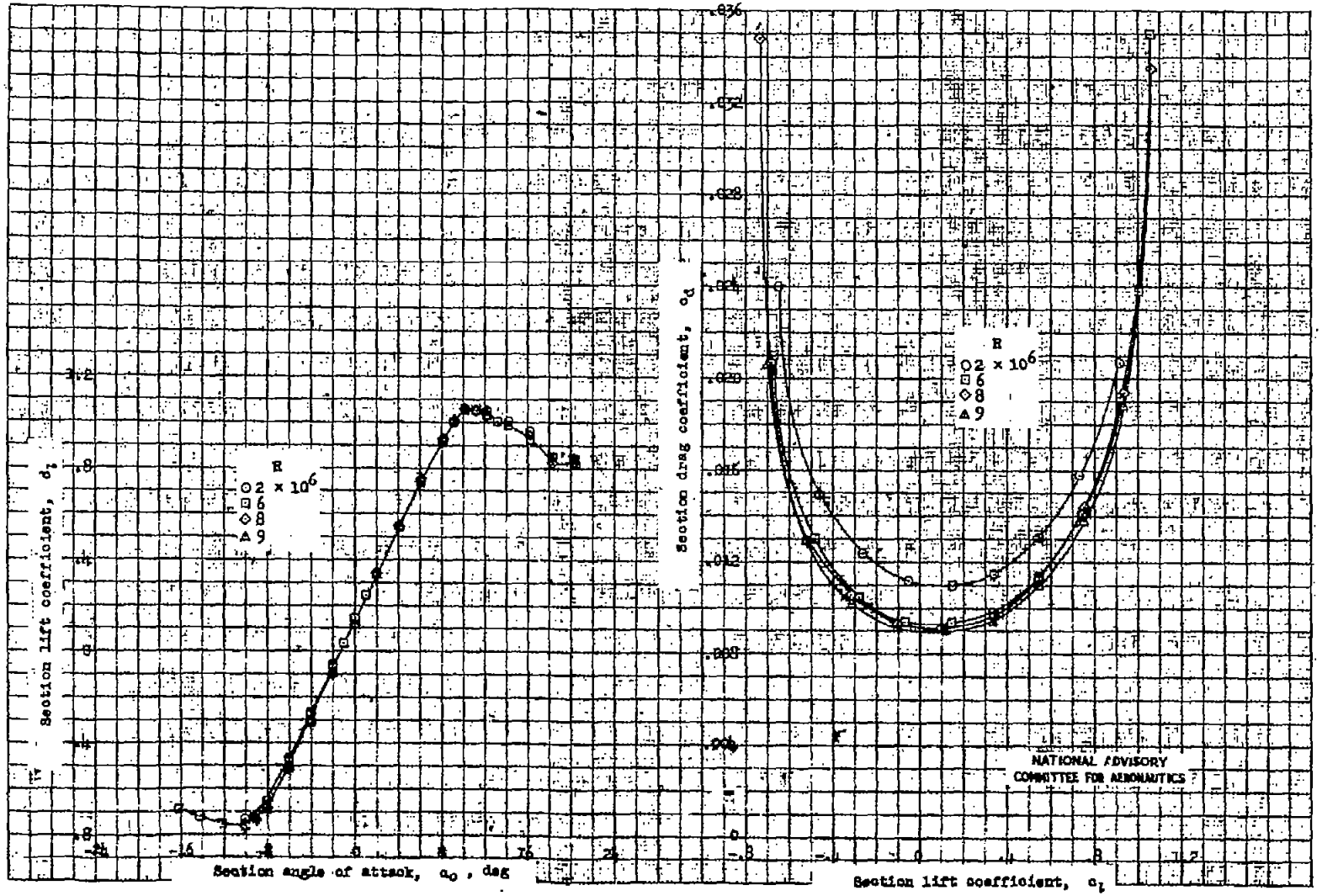

(b) Standard leading-edge roughness.

Figure 9 .- Concluded.

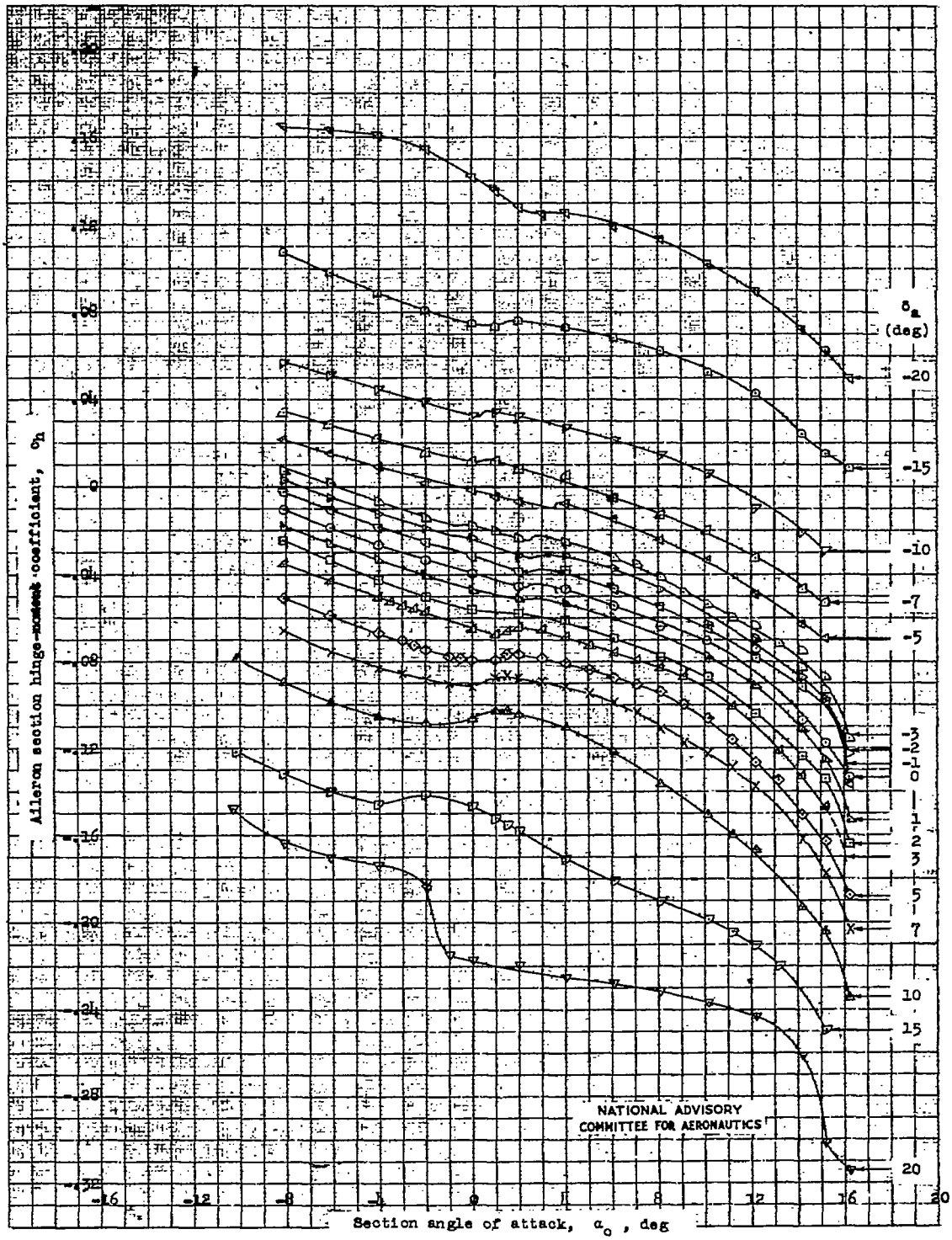

(a) Smooth condition.

Figure 10.- Hinge-moment characteristics of a sealed 0.22c internally balanced aileron of modified contour on an NACA $65_{(112)}$-213 airfoil section. $R = 8 \times 10^6$; tests, TDT 709 and 711.

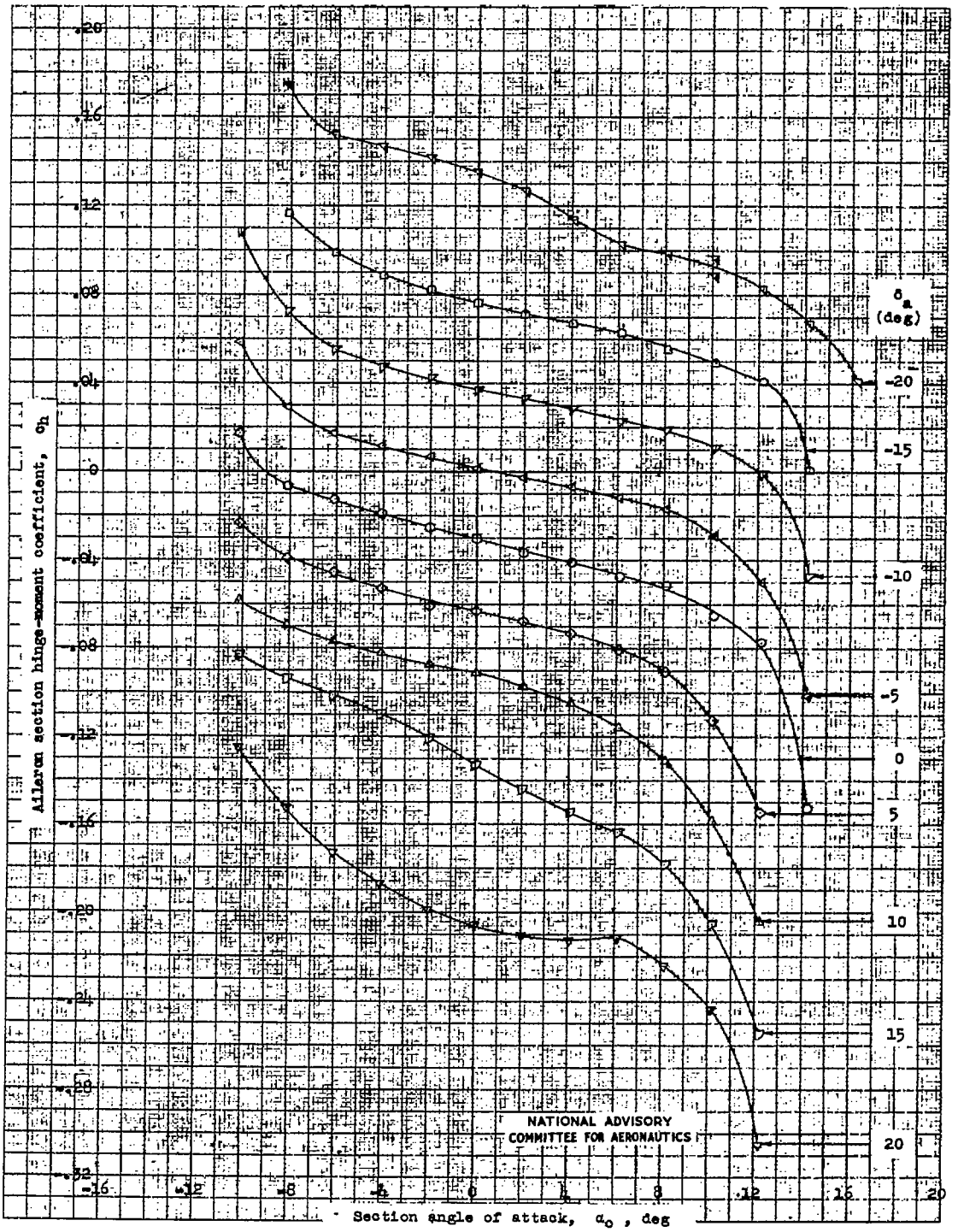

(b) Standard leading-edge roughness.

Figure 10.- Concluded.

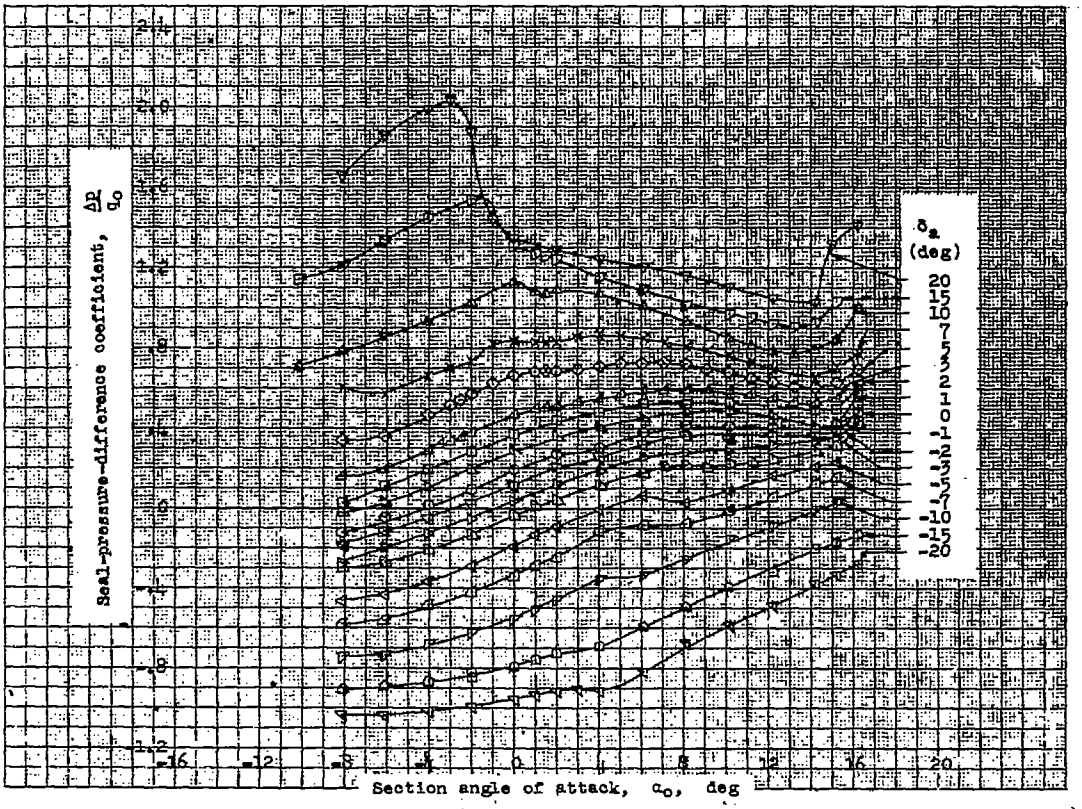

(a) Smooth condition.

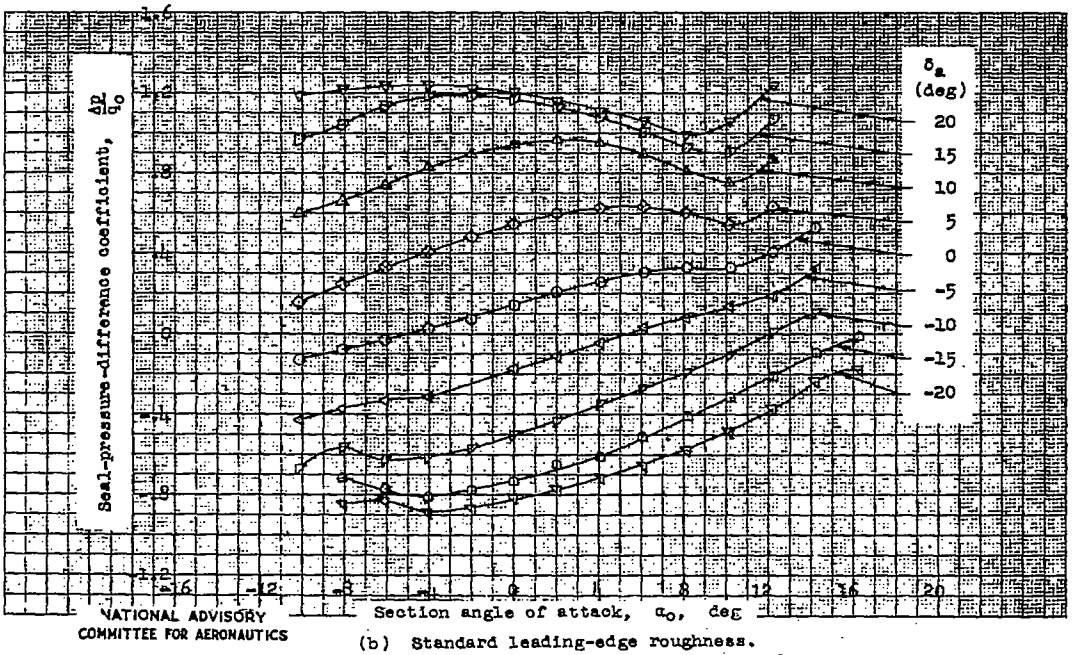

(b) Standard leading-edge roughness.

Figure 11.- Variation of $\frac{\Delta p}{q_o}$ with α_o for a sealed 0.22c internally balanced aileron of modified contour on an NACA $65_{(112)}$-213 airfoil section. $R = 8 \times 10^6$; tests, TDT 709 and 711.

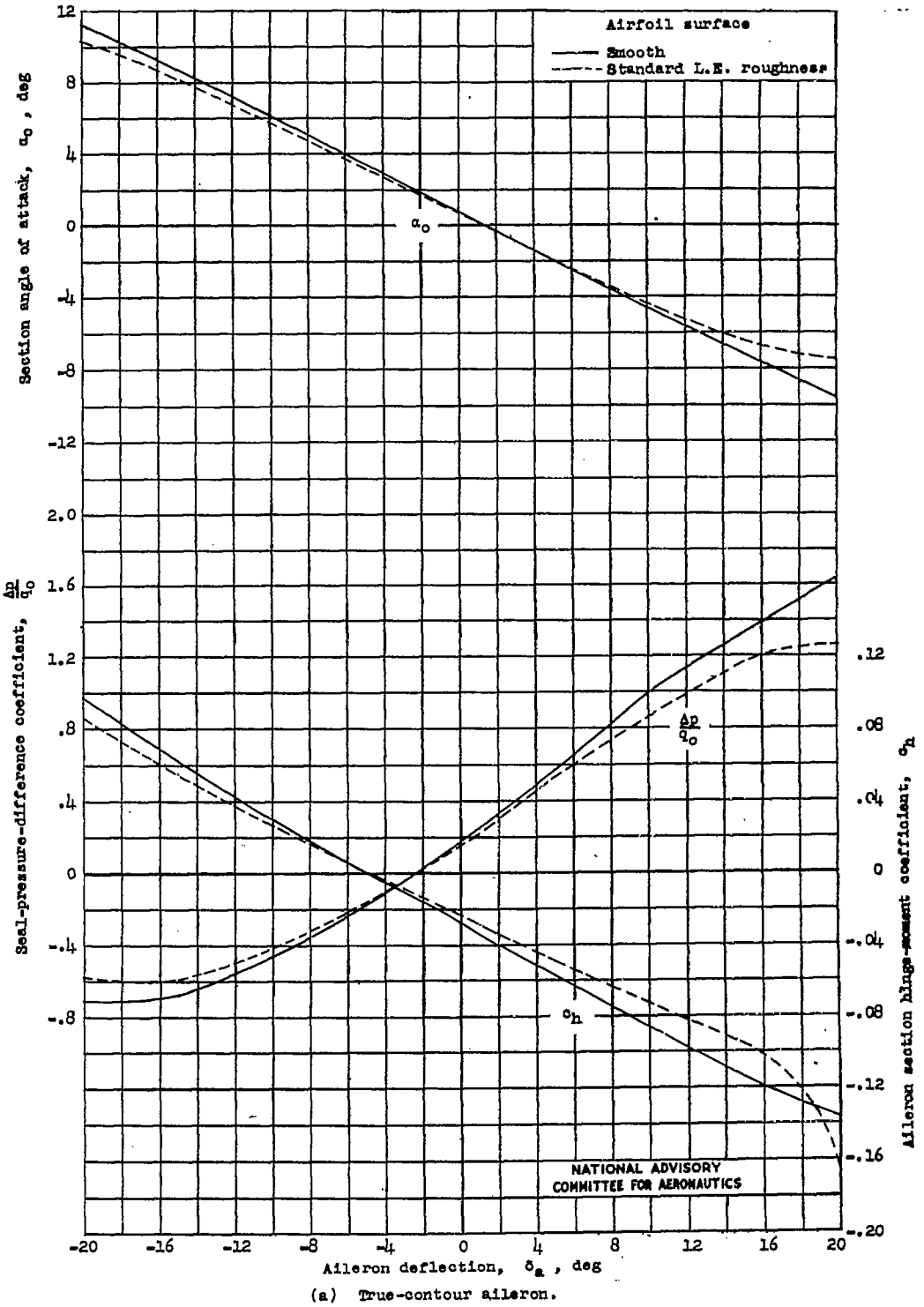

(a) True-contour aileron.

Figure 12.- Variation of aerodynamic characteristics with aileron deflection at a constant section lift coefficient of 0.20 for an NACA $65_{(112)}$-213 airfoil section equipped with two interchangeable sealed 0.22c internally balanced ailerons of different contour. $c_b = 0.33c_a$; $R = 8 \times 10^6$.

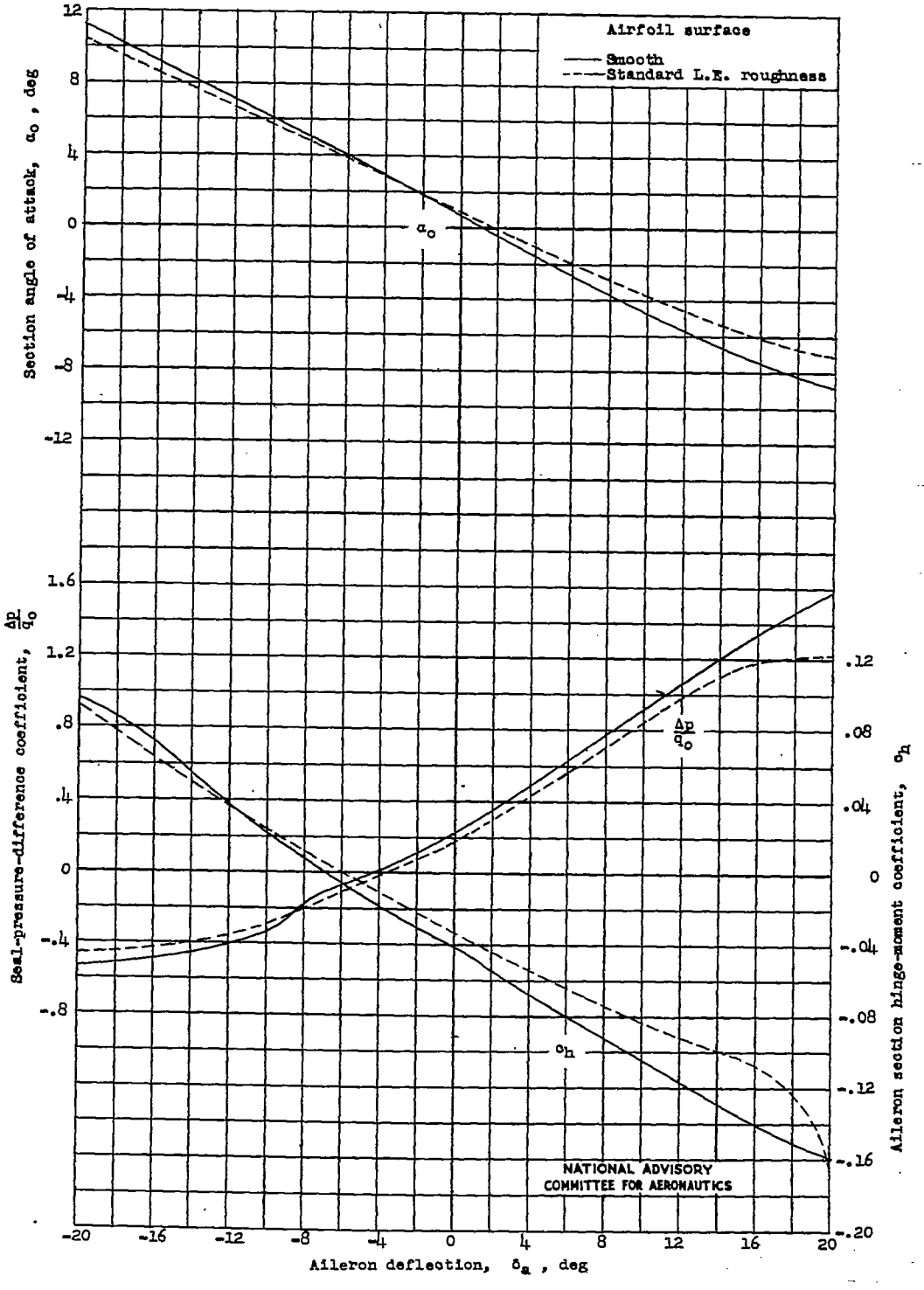

(b) Modified aileron.

Figure 12.- Concluded.

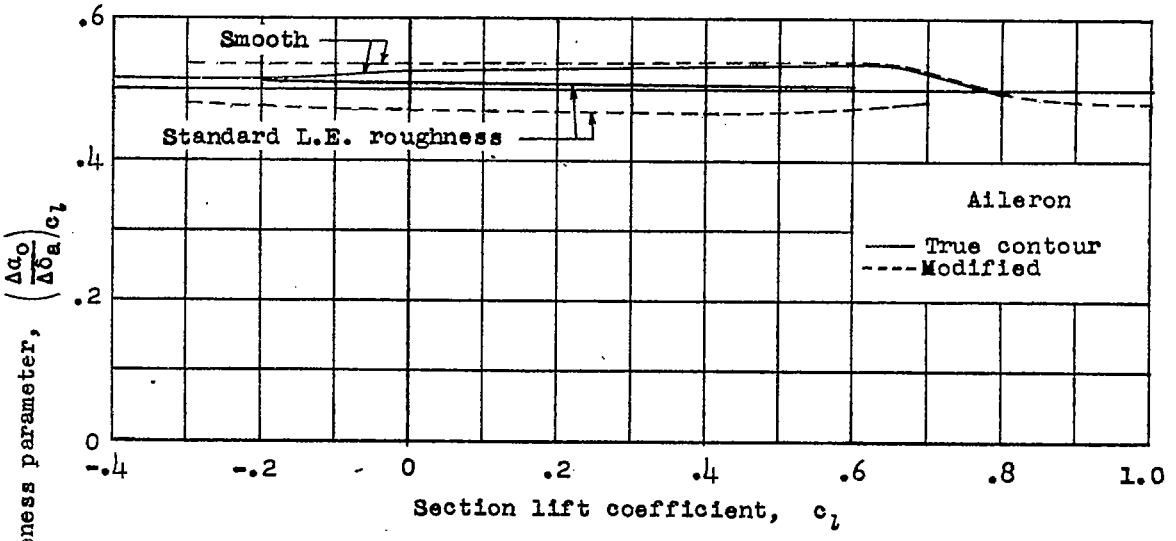

(a) $-10^\circ < \delta_a < 10^\circ$.

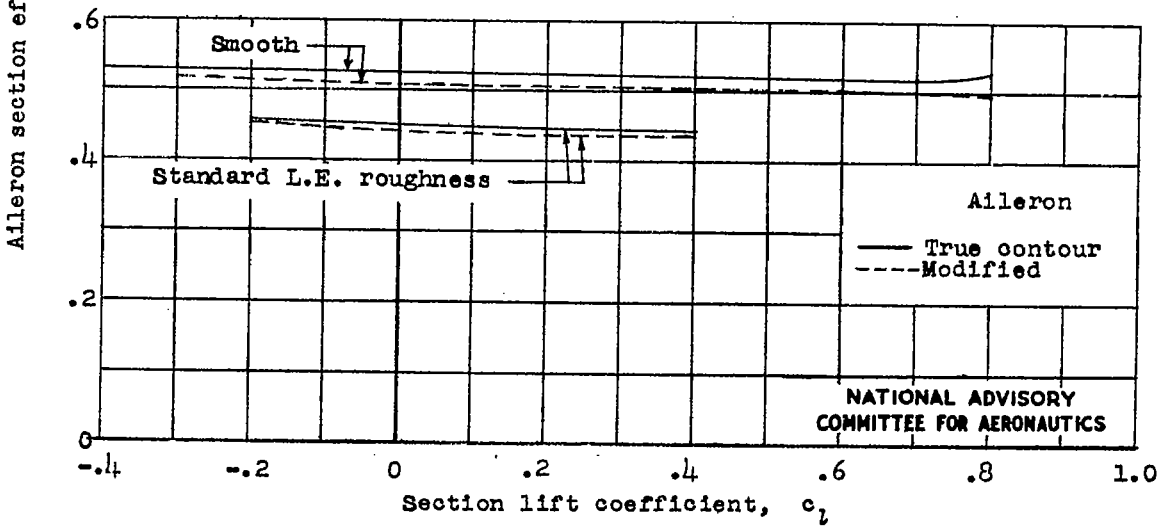

(b) $-20^\circ < \delta_a < 20^\circ$.

Figure 13.- Variation of $\left(\frac{\Delta a_0}{\Delta \delta_a}\right)_{c_l}$ with c_l for an NACA $65_{(112)}$-213 airfoil section equipped with a sealed 0.22c internally balanced aileron. $R = 8 \times 10^6$.

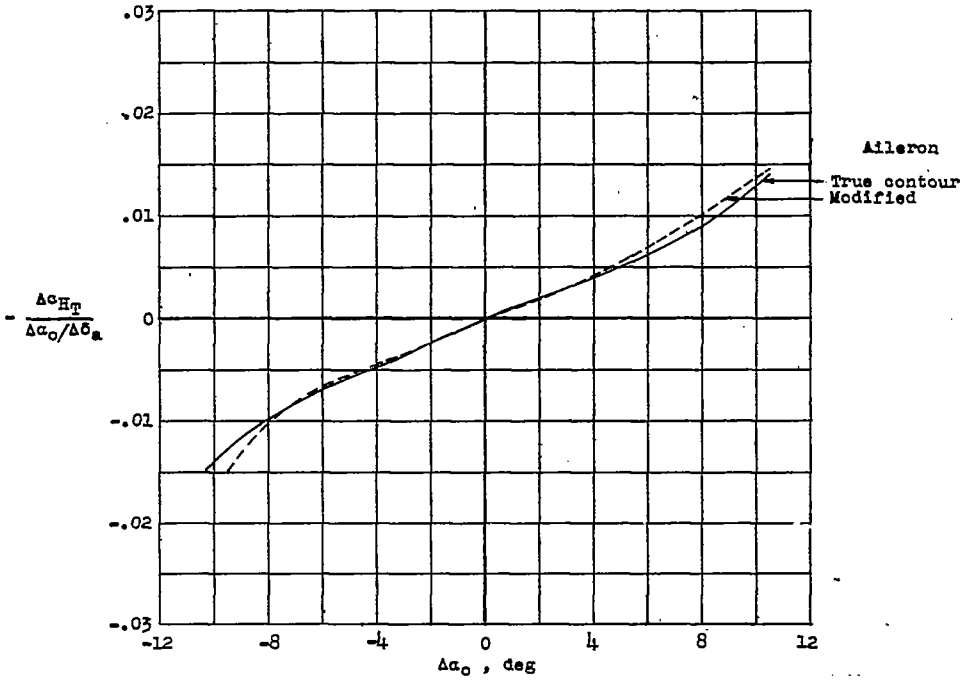

(a) Smooth airfoil.

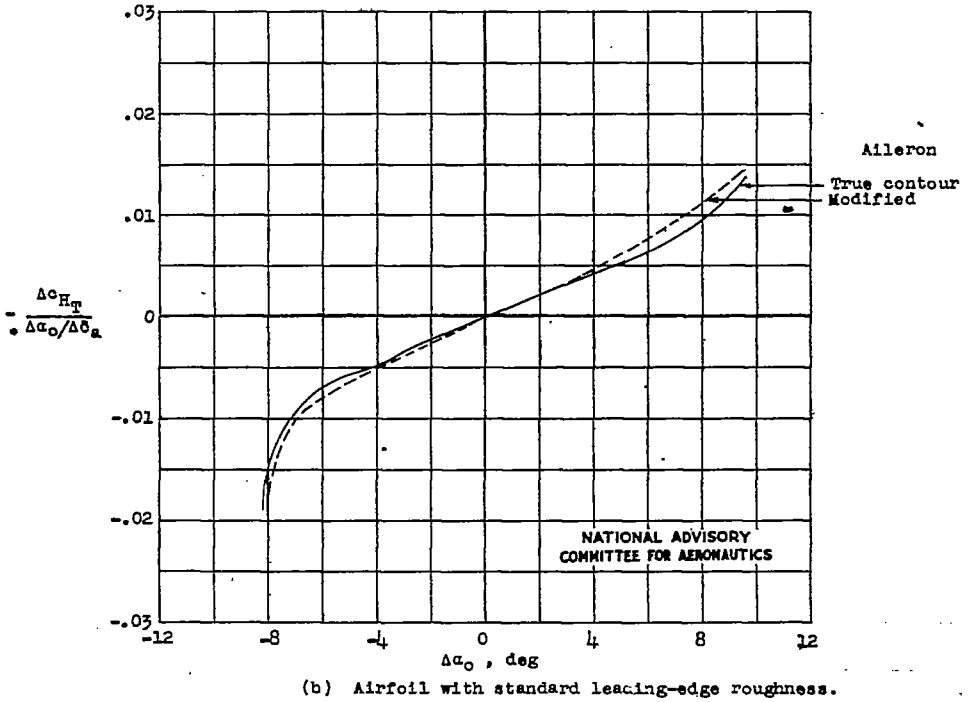

(b) Airfoil with standard leading-edge roughness.

Figure 14.- Variation of the hinge-moment parameter $\frac{\Delta c_{H_T}}{\Delta\alpha_o/\Delta\delta_a}$ with equivalent change in section angle of attack required to maintain a constant section lift coefficient of 0.20 for deflection of sealed 0.22c internally balanced ailerons of different contours on an NACA $65_{(112)}$-213 airfoil section. $R = 8 \times 10^6$.

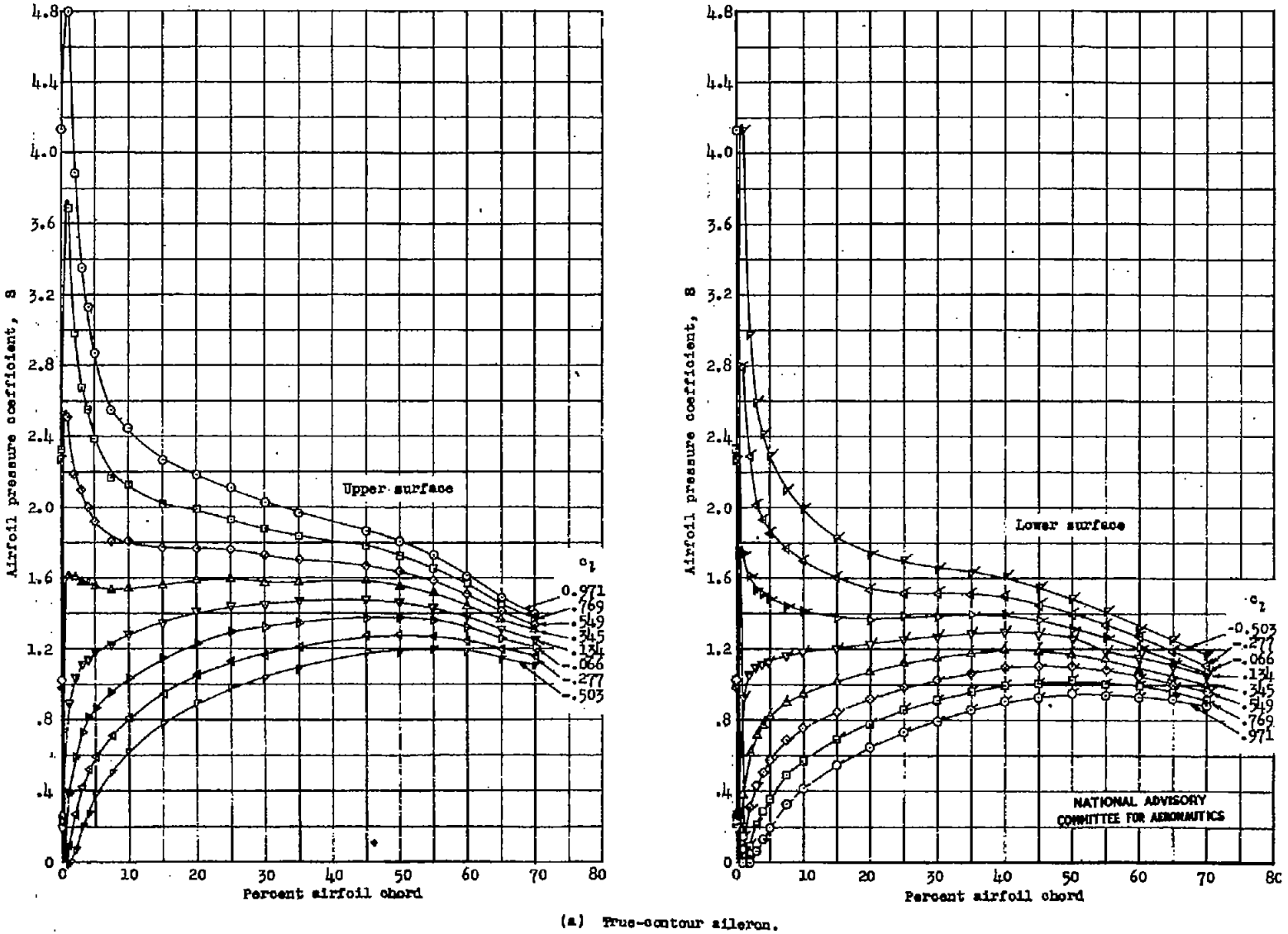

(a) True-contour aileron.

Figure15.- Experimental pressure distributions for an NACA $65_{(112)}$-213 airfoil section equipped with a sealed 0.22c internally balanced aileron. $\delta_a = 0°$; tests, TDT 704, 707, and 714.

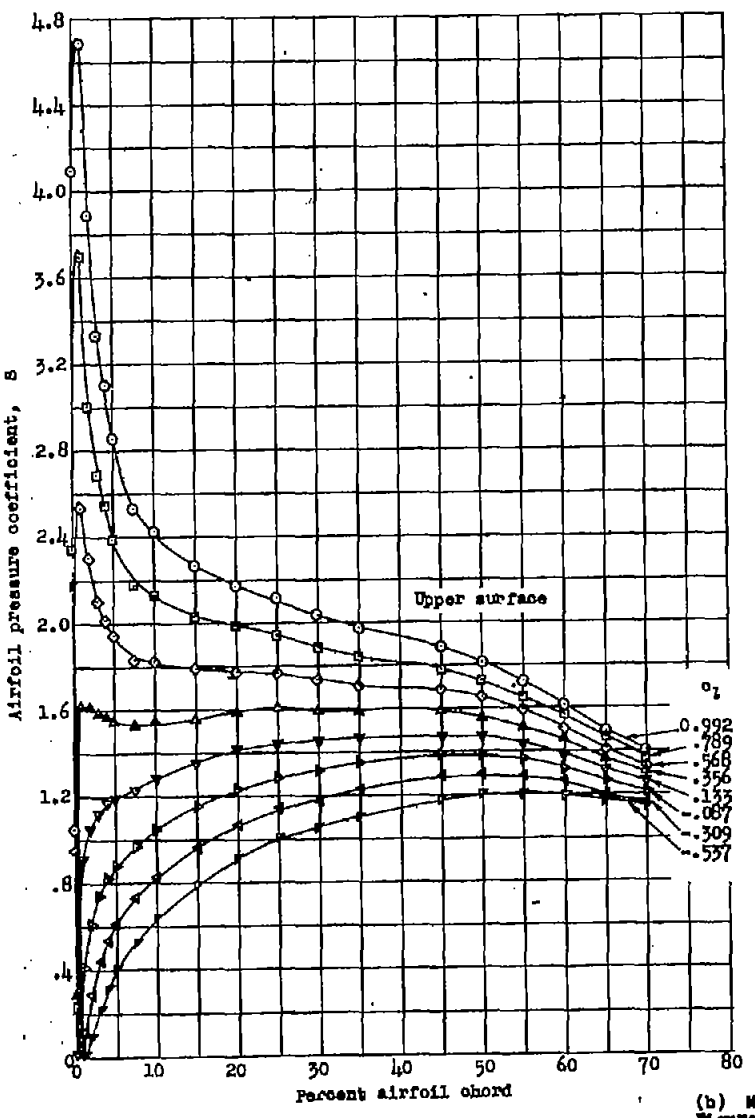

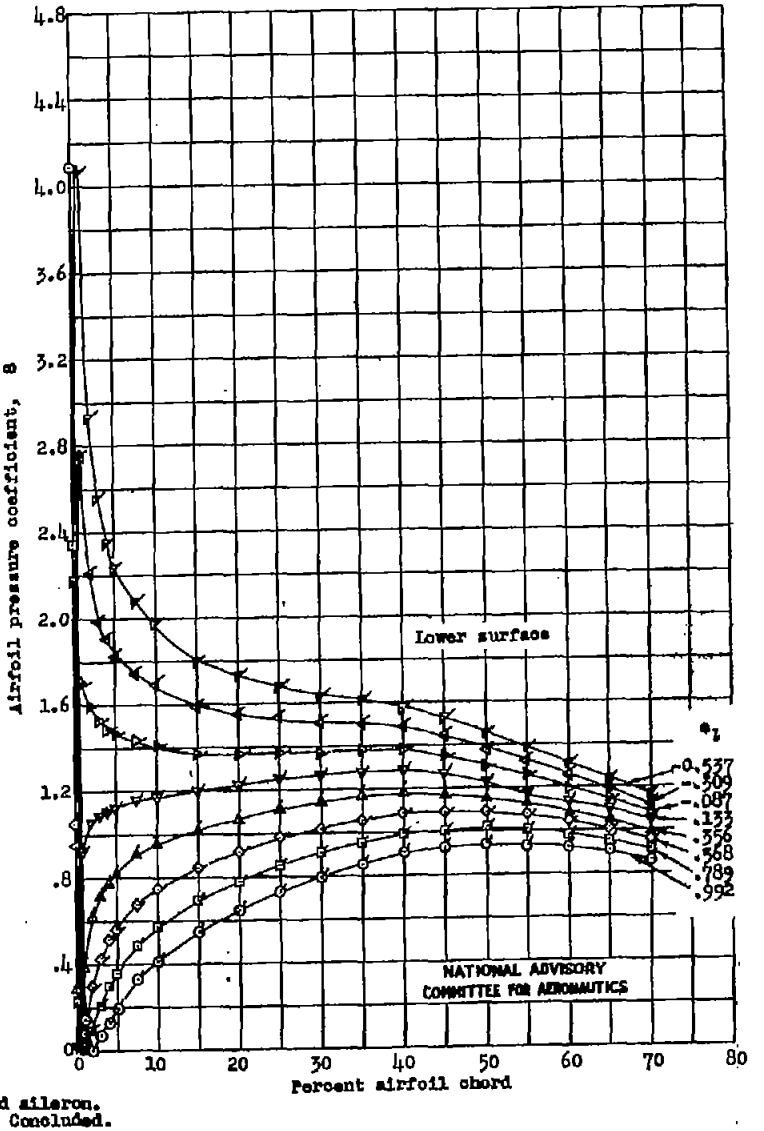

(b) Modified aileron.

Figure 15.- Concluded.

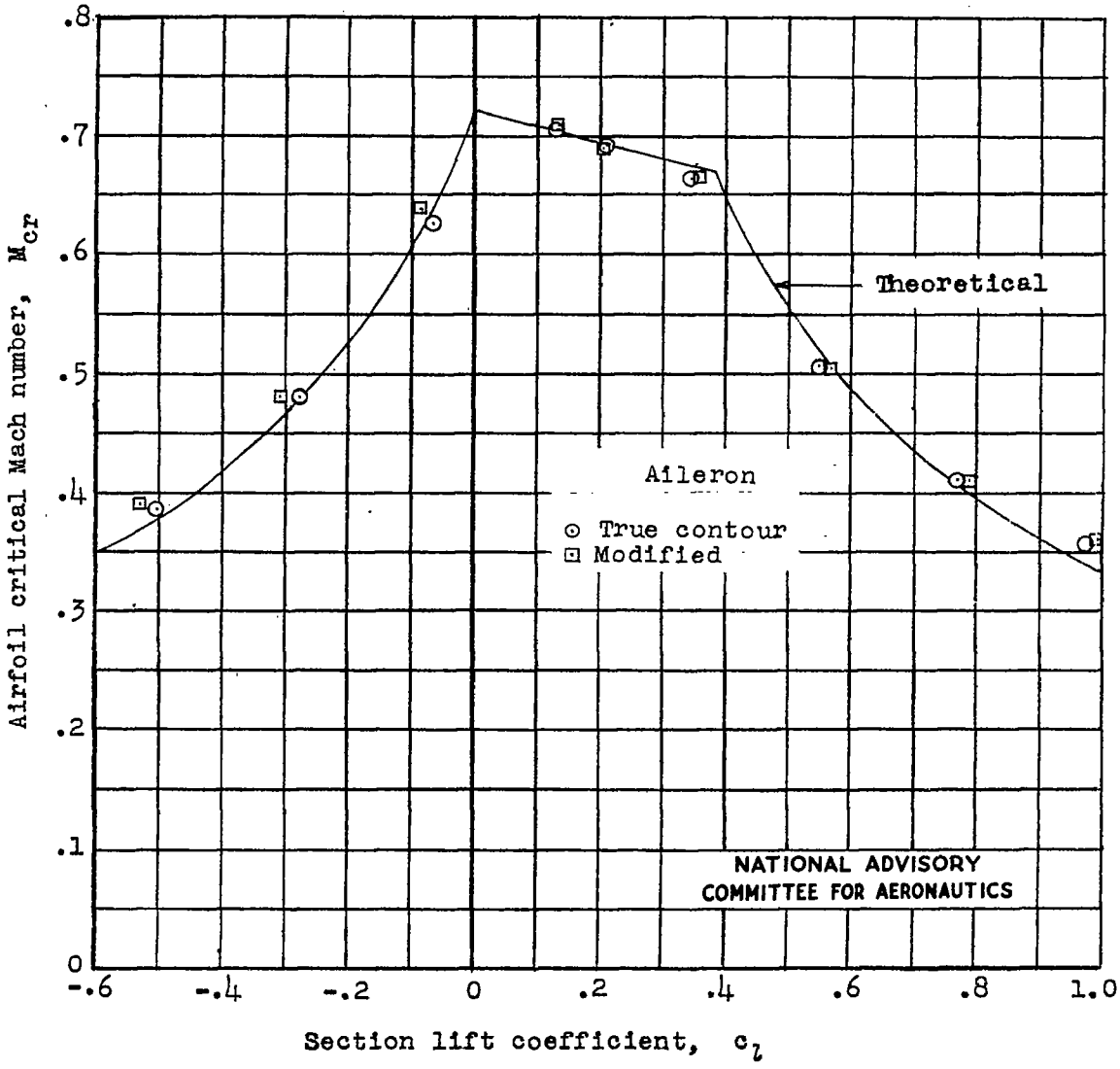

Figure 16.- Variation of predicted critical Mach number with low-speed section lift coefficient for an NACA $65_{(112)}$-213 airfoil section equipped with a sealed 0.22c internally balanced aileron. $\delta_a = 0°$.

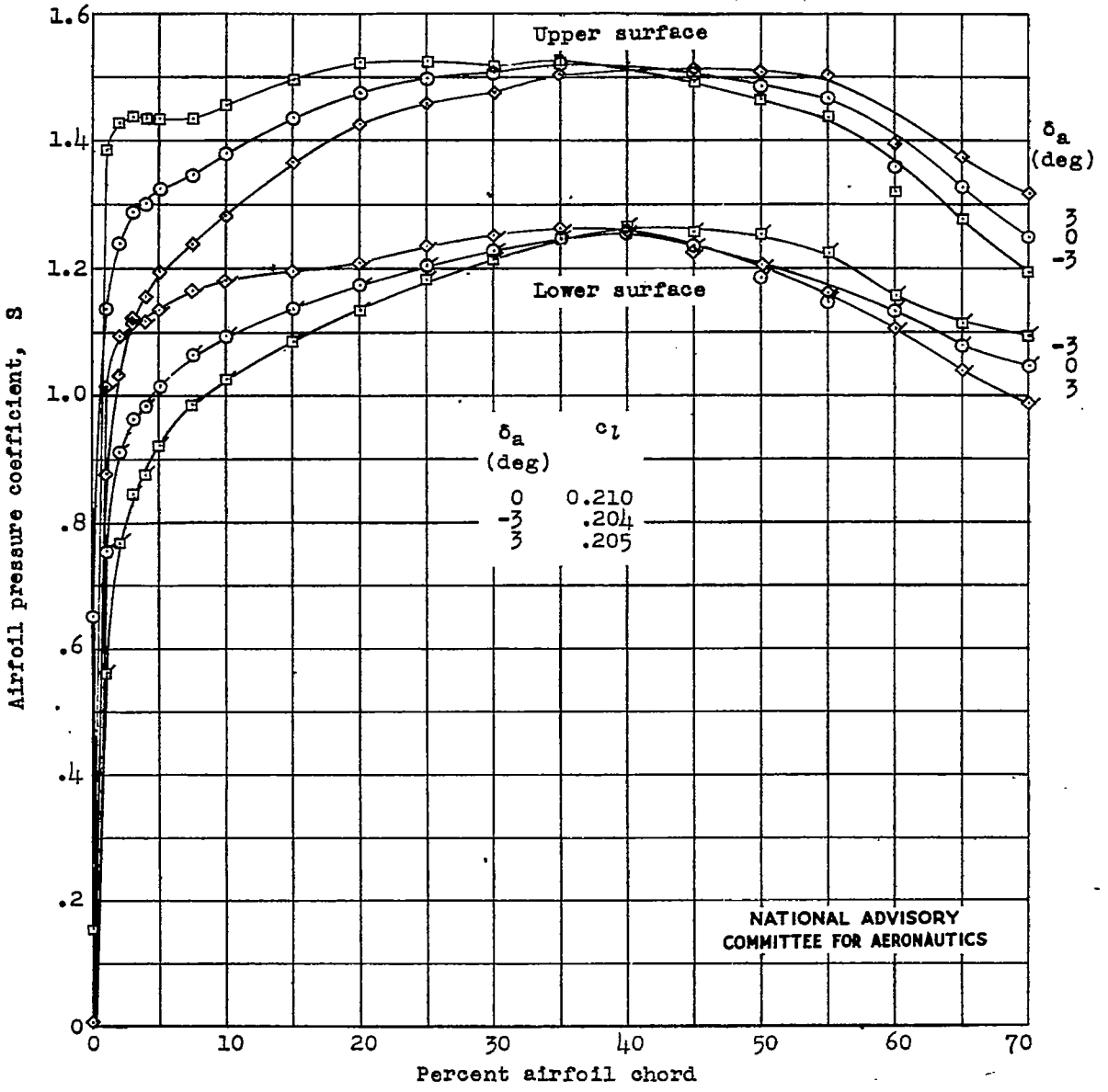

(a) True-contour aileron.

Figure 17.- Experimental pressure distributions for an NACA $65_{(112)}$-213 airfoil section equipped with a sealed 0.22c internally balanced aileron. Tests, TDT 704 and 714.

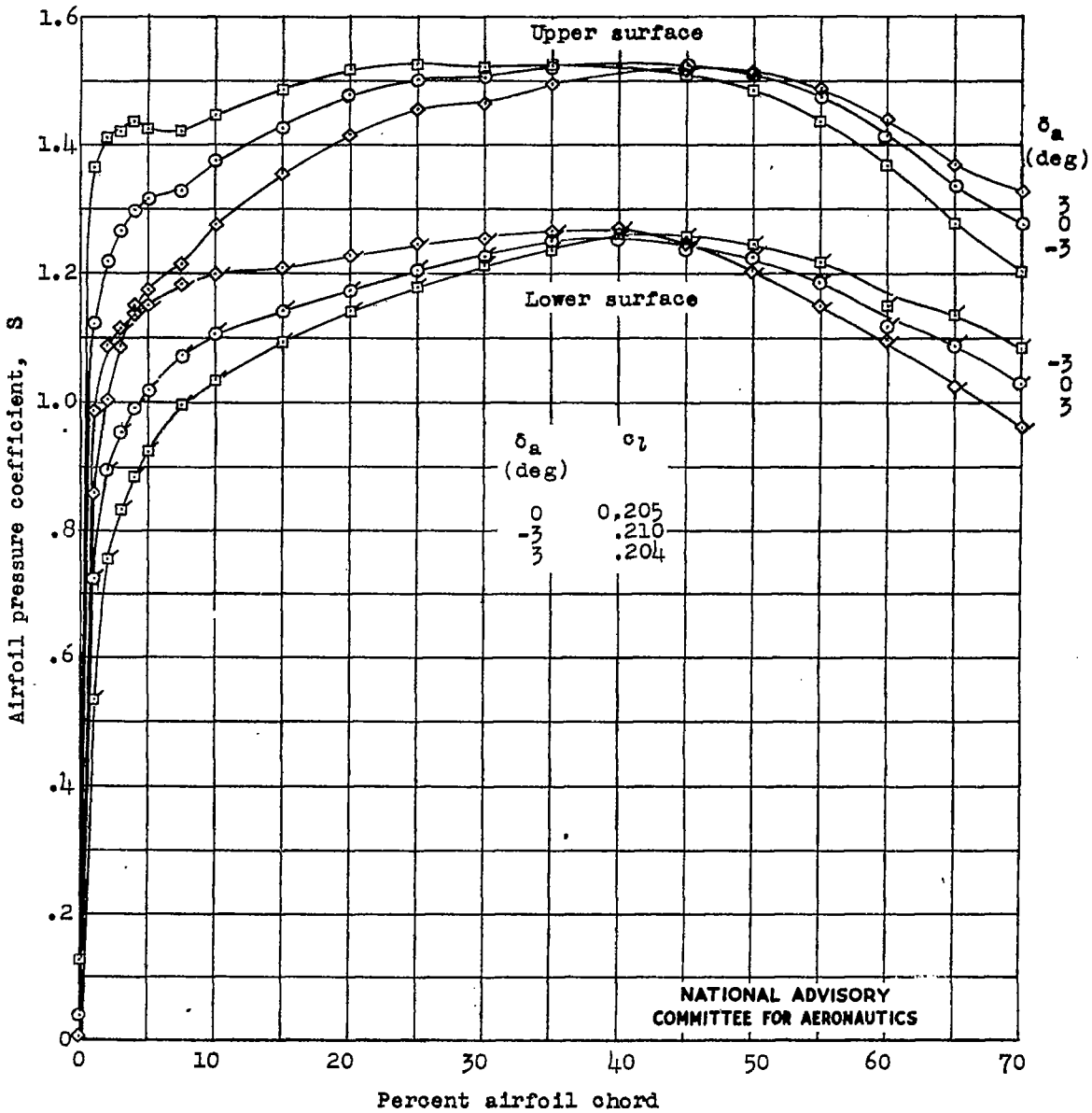

(b) Modified aileron.

Figure 17.- Concluded.